

1 **Dissolved Inorganic Nutrients in the Western Mediterranean Sea (2004-2017)**

2 Malek Belgacem^{1,2}, Jacopo Chiggiato^{1,*}, Mireno Borghini¹, Bruno Pavoni², Gabriella Cerrati³,
3 Francesco Aciri¹, Stefano Cozzi⁴, Alberto Ribotti⁵, Marta Álvarez⁶, Siv K. Lauvset⁷, Katrin Schroeder¹

4 ¹ CNR-ISMAR, Arsenale Tesa 104, Castello 2737/F, 30122 Venezia, Italy

5 ² Dipartimento di Scienze Ambientali Informatica e Statistica, Università Ca' Foscari Venezia,
6 Campus Scientifico Mestre, Italy

7 ³ ENEA, Department of Sustainability, S. Teresa, Marine Environmental center, 19032 Pozzuolo di
8 Lerici (SP), Italy

9 ⁴ CNR-ISMAR, Area Science Park – Basovizza, 34149 Trieste, Italy

10 ⁵ CNR-IAS, Loc. Sa Mardini snc, Torregrande, 9170 Oristano, Italy

11 ⁶ Instituto Español de Oceanografía, IEO, A Coruña, Spain

12 ⁷ NORCE Norwegian Research Centre, Bjerknes Centre for Climate Research, 5007 Bergen, Norway

13 *Corresponding author's email: jacopo.chiggiato@ismar.cnr.it

15 **Abstract**

16 Long-term time-series are a fundamental prerequisite to understand and detect climate shifts and
17 trends. Understanding the complex interplay of changing ocean variables and the biological
18 implication for marine ecosystems requires extensive data collection for monitoring, hypothesis testing
19 and validation of modelling products. In marginal seas, such as the Mediterranean Sea, there are still
20 monitoring gaps, both in time and in space. To contribute to filling these gaps, an extensive dataset of
21 dissolved inorganic nutrient observations (nitrate, phosphate, Si and silicate) has been collected
22 between 2004 and 2017 in the Western Mediterranean Sea and subjected to rigorous quality control
23 techniques to provide to the scientific community a publicly available, long-term, quality controlled,
24 internally consistent biogeochemical data product. The data product includes 870 stations of dissolved
25 inorganic nutrients, including temperature and salinity, sampled during 24 cruises. Details of the
26 quality control (primary and secondary quality control) applied are reported. The data are available in
27 PANGAEA (<https://doi.pangaea.de/10.1594/PANGAEA.904172>, Belgacem et al. 2019)

28 **Keywords:** Mediterranean Sea, Dissolved Inorganic Nutrient, biogeochemistry.

29

30 **1 Introduction**

31 Dissolved inorganic nutrients play a crucial role in marine ecosystem functioning. They serve as
32 regulators of ocean biological productivity, and are trace elements for biogeochemical cycling as well
33 as for natural and anthropogenic sources and transport processes (Bethoux, 1989; Bethoux et al.,
34 1992). They are also non-conservative tracers, since their distribution vary according to both
35 biological (such as primary production and respiration) and physical (such as convection, advection,
36 mixing and diffusion) processes. Very schematically, inorganic nutrients are continuously consumed
37 by phytoplankton (due to primary production) in the sea surface and regenerated in the mesopelagic
38 layer by bacteria and animals (due to respiration). Moreover, the sinking of organic matter and its
39 decomposition increases the nutrient concentrations in the intermediate and deep-water masses over
40 time. To identify the limiting factors for biological production in the oceans, we need to understand
41 the underlying chemical constraints and especially the macro- and micronutrients spatial and temporal
42 variations. Dissolved inorganic nutrients may be used as tracers of water masses like salinity and
43 temperature, to assess mixing processes, and to understand the biogeochemical circumstances of their
44 formation regions. Understanding the complex interplay of changing ocean variables and the
45 biological implication for marine ecosystems is a difficult task and requires not only modelling, but
46 also extensive data collection for monitoring, hypothesis testing and validation. Monitoring gaps still
47 remain in both in time and space, especially for marginal seas such as the Arctic Ocean or the
48 Mediterranean Sea.

49 The Mediterranean Sea has been identified as a region significantly affected by ongoing climatic
50 changes, like warming and decrease in precipitation (Giorgi, 2006). In addition, it is a region
51 particularly valuable for climate change research because it behaves like a miniature ocean (Bethoux

52 et al., 1999) with a well-defined overturning circulation characterized by spatial and temporal scales
53 much shorter than for the global ocean, with a turnover of only several decades. Being an
54 intercontinental sea, and subjected to more terrestrial nutrient inputs (river runoff, submarine
55 groundwater discharge) and atmospheric deposition, the Mediterranean Sea has a nitrate to phosphate
56 N:P ratio that is anomalously high compared to the “classical” world's oceans Redfield ratio,
57 indicating a general P-limitation regime, which becomes stronger along a west-to-east gradient. The
58 Mediterranean Sea is therefore a potential model to study global patterns that will be experienced in
59 the next decades worldwide, not only regarding ocean circulation, but also the marine biota (Lejeune
60 et al., 2010). Several environmental variables can act as stressors for marine ecosystems, by which
61 climatically driven ecosystem disturbances are generated (Boyd, 2011). These changes affect, among
62 others, the distribution of biogeochemical elements (including inorganic nutrients) and the functioning
63 of the biological pump and CO₂ regulation.

64 Within this context, the aim of this paper is to compile an extensive dataset of dissolved inorganic
65 nutrient observations (nitrate, phosphate, and silicate) collected between 2004 and 2017 in the
66 Western Mediterranean Sea (WMED), to describe the quality control techniques and to provide the
67 scientific community with a publicly available, long-term, quality controlled, and internally consistent
68 biogeochemical data product, contributing to previously published Mediterranean Sea datasets like the
69 MEDAR/Medatlas (time period:1908–1999), (Fichaut et al., 2003) and the Mediterranean Sea –
70 Eutrophication and Ocean Acidification aggregated datasets v2018 (time period: 1911-2017) provided
71 by EMODnet Chemistry (Giorgetti al.,2018) available at
72 <https://www.seadatanet.org/Products/Aggregated-datasets>.

73 Both original and quality-controlled data are available in PANGAEA:

74 <https://doi.pangaea.de/10.1594/PANGAEA.904172>

75 Coverage: 44°N-35°S; 6°W-14°E

76 Location Name: Western Mediterranean Sea

77 Date start: May 2004

78 Date end: November 2017

79 **2 Dissolved inorganic nutrient data collection**

80 **2.1. The CNR dissolved inorganic nutrient data in the WMED**

81 Long-term time-series, such as the OceanSites global time series (www.oceansites.org), are a
82 fundamental prerequisite to understand and detect climate shifts and trends. However, biogeochemical
83 time-series are still limited to the northern Western Mediterranean Sea (MOOSE network, Coppola et
84 al., 2019). Yet, inorganic nutrients in the Mediterranean Sea has received more attention in recent
85 years, and various datasets have been compiled to understand its unique characteristics such as the one
86 build by the PERSEUS project Consortium (“Policy-oriented marine environmental research in the
87 southern European seas” - EU FP7 project GA #287600), that included 100 cruises collected during
88 the project’s lifetime, in addition to those from other projects like SESAME, EU FP7 project GA
89 #GOCE-036949), and data products such as the MEDAR/Medatlas. In addition to that, the data
90 assembly system EMODnet Chemistry, a leading infrastructure supported by pan-European directorate
91 General MARE set up (Martin Miguez et al., 2019, Tintoré et al.,2019).

92 The dataset presented here consists of 24 oceanographic cruises (Fig. 1, Table 1a and Table 1b)
93 conducted in the WMED on board of research vessels run by the Italian National Research Council
94 (CNR) and the Science and Technology Organisation Centre for Maritime Research and
95 Experimentation (NATO-STO CMRE). All cruises were merged into a unified dataset with 870
96 nutrient stations and ~ 9666 data points over a period of 13 years (2004-2017). The overall spatial
97 distribution of the stations covers the whole WMED, but the actual distribution strongly varies
98 depending on the specific cruise and most of the data are collected along sections. At all stations,
99 pressure, salinity and temperature were measured with a CTD-rosette system consisting of a CTD SBE
100 911 plus and a General Oceanics rosette with 24 12L Niskin Bottles. Temperature measurements were

101 performed with the SBE-3/F thermometer with a resolution of 10^{-3} °C; conductivity measurements
102 were performed with the SBE-4 sensor with a resolution of $3 \cdot 10^{-4}$ S/m. The probes were calibrated
103 before and after each cruise. During all CNR cruises, redundant sensors were used for both
104 temperature and salinity measurements.

105 Seawater samples for dissolved inorganic nutrient measurements were collected during the CTD up-
106 cast at standard depths (with slight modifications according to the depth at which the deep chlorophyll
107 maximum was detected). The standard depths are usually 5, 25, 50, 75, 100, 200, 300, 400, 500, 750,
108 1000, 1250, 1500, 1750, 2000, 2250, 2500, 2750, 3000 m. No filtration was employed, nutrient
109 samples were immediately stored at -20 °C. Note that sample storage and freezing duration varied
110 greatly from one cruise to another (Table 3 shows cruises where this exceeded 1 year).

111 **2.2. Analytical methods for inorganic nutrients**

112 For all cruises, nutrient determination (nitrate, orthosilicate and orthophosphate) was carried out
113 following standard colorimetric methods of seawater analysis, defined by Grasshoff et al. (1999) and
114 Hansen and Koroleff (1999). For inorganic phosphate, the method is based on the reaction of the ions
115 with an acidified molybdate reagent to yield a phosphomolybdate heteropoly acid, which is then
116 reduced to a blue-colored compound (absorbance measured at 880 nm). Inorganic nitrate is reduced
117 (with cadmium granules) to nitrite that react with an aromatic amine leading to the final formation of
118 the azo dye (measured at 550 nm). Then, the nitrite separately determined must be subtracted from the
119 total amount measured to get the nitrate concentration only. The determination of dissolved silicon is
120 based on the formation of a yellow silicomolybdic acid reduced with ascorbic acid to blue-colored
121 complex (measured at 820 nm).

122 Nutrient analysis was performed in three laboratories. From 2004 to 2013, all cruises nutrients were
123 analysed by ENEA, while for those of 2015 (cruise #23) and 2017 (cruise #24), nutrient
124 concentrations were analysed by CNR-ISMAR. Referring to Table 1S, four different models of

125 autoanalyzer were used. Measurements from the autoanalyzer were reported in $\mu\text{mol L}^{-1}$. Inorganic
126 nutrient concentrations were converted to the standard unit $\mu\text{mol kg}^{-1}$, using sample salinity from CTD
127 and a mean laboratory analytical temperature of 20°C. Data from nutrient analysis were then merged
128 to ancillary CTD bottle data.

129 **2.3. Reference inorganic nutrient data**

130 In addition to the data collected during the above-mentioned cruises, and in order to perform the
131 secondary quality control (described below), we identified five reference cruises (Table 2), based on
132 their spatial and temporal distribution and the reliability of the measurements (see Fig. 2 –Table.3S
133 Fig.1S). Cruises 06MT20110405 and 06MT20011018 are the only two Mediterranean cruises included
134 in the publicly available Global Ocean Data Analysis Project version 2 (GLODAPv2, Olsen et al.
135 2016). These cruises, conducted on board the R/V Meteor, provide a reliable reference because
136 nutrient analysis strictly followed the recommendation of the World Ocean circulation experiment
137 (WOCE) and the GO-SHIP protocols (Hydes et al., 2010; ,Tanhua et al., 2013). Cruises
138 29AH20140426 and 48UR20070528 are to be included in the CARIMED data product (personal
139 communication by M. Álvarez, in preparation but not yet available) and have undergone rigorous
140 quality control following GLODAP routines. Finally, 29AJ20160818 was carried out in the framework
141 of the MedSHIP programme (Schroeder et al., 2015) and its data are available at
142 <https://doi.org/10.1594/PANGAEA.902293> (Tanhua, 2019).

143 **3 Quality Assurance and quality control methods**

144 Combining inorganic nutrient data from different sources, collected by different operators, stored for
145 different amounts of time, and analysed by multiple laboratories, is not a straightforward task. This is
146 widely recognized in the biogeochemical oceanographic community. Since the 1990s, several studies
147 and programmes (e.g. World Ocean Database, World Ocean Atlas, WOCE) have been devoted to
148 facilitate the exchange of oceanographic data and develop quality control procedures to compile

149 databases by the estimation of systematic errors (Gouretski and Jancke, 2000) to increase the inter-
150 comparability, generate consistent data sets and accurately observe the long-term change.

151 An example of a first quality control procedure is the use of reference materials that are available for
152 salinity (IAPSO, salinity standard by OSIL) and temperature (SPRT, Standard Platinum Resistance
153 Thermometer). As for the inorganic carbon, total alkalinity (Dickson et al., 2003) and inorganic
154 nutrients (Aoyama et al., 2016), certified reference materials (CRM) have been recently made
155 applicable for oceanographic cruises. However, since CRM are not always available or used for
156 biogeochemical oceanographic data, Lauvset and Tanhua (2015) developed a secondary quality
157 control tool to identify biases in deep data. The method suggests adjustments that reduce cruise to
158 cruise biases, increase accuracy and allow for the inter-comparison between data from various sources.
159 This approach, based on a crossover and inversion method (Gouretski and Jancke, 2000; Johnson et
160 al., 2001), was used to generate the CARbon IN Atlantic ocean (CARINA, see Hoppema et al., 2009),
161 GLODAPv2.2019 (Olsen et al., 2019) and PACIFICA (Suzuki et al., 2013) data products.

162 **3.1 Primary Quality control**

163 Each individual cruise was first subjected to a primary quality control (1st QC) that included a check of
164 apparent and extreme outliers in CTD salinity, nitrate, phosphate and silicate. Each parameter included
165 a quality control flag, following standard WOCE flags (Table 3). Surface, intermediate and deep layer
166 were evaluated separately because nutrient observations evolve differently in each layer. The
167 coefficient of variation (CV, defined as standard deviation over mean) was computed for each depth
168 layer. Coefficients of variation in the surface (0-250 db) layer were high (nitrate CV=1.16, phosphate
169 CV=1.005, silicate CV=0.75) due to air-sea interaction (Muniz et al., 2001) occurring in this layer
170 rendering it difficult to flag. These influences are of reduced importance in the intermediate (250-1000
171 db) layer (nitrate CV=0.23, phosphate CV=0.31, silicate CV=0.24) and the deep (>1000 db) layer
172 (nitrate CV=0.15, phosphate CV=0.22, silicate CV=0.14), decreasing the total variance. Flags in the
173 upper and intermediate layer were thus set based on outliers within pressure ranges defined according

174 to standard pressures (0-10, 10-30, 30-60, 60-80, 80-160, 160-260, 260-360, 360-460, 460-560, 560-
175 1000 db).

176 Below 1000 db, flagging included an inspection of nitrate to phosphate (N:P) and nitrate to silicate (N:
177 Si) ratios. The Median and Median Absolute Deviation (MAD) was computed by classes of pressure:
178 we considered as outlier any atypical observation and any value that departs from the median by more
179 than three MADs in the different pressure ranges for each cruise.

180 An overview of the nutrient distribution is provided with scatter plots, showing also the flagged
181 measurements (Fig. 3). Each measurement was flagged 2 (“Acceptable/ measured”) or flagged 3
182 (“Questionable”): 4.1% of nitrate data, 3.37% of phosphate data, 3.16% of silicate data, and 0.07% of
183 CTD salinity data were considered outliers and flagged 3. As highlighted by Tanhua et al. (2010), the
184 primary QC can be subjective depending on the expertise of the person flagging the data, thus flagging
185 could bring in some uncertainties.

186 In order to have a first assessment of the precision of each cruise measurements, the standard deviation
187 of observations deeper than 1000 db was calculated along with averages and standard deviations for
188 each cruise and by subregions to have an overview about nutrient content variability in the deep layer
189 and about the observations spatial spread of individual cruises (Table 4). Following the subdivision of
190 Manca et al. (2004), the WMED has been divided into subregions (Fig.2S, Table 2S) according to the
191 general circulation patterns (details in Manca et al.,2004). Table 4 displays the comparison of standard
192 deviation of deep measurements for each cruise and within subregions. The overall standard deviation
193 between cruises in the deep layer varied between 0.51 and 1.41 $\mu\text{mol kg}^{-1}$ for nitrate, between 0.1 and
194 1.64 $\mu\text{mol kg}^{-1}$ for silicate and between 0.025 and 0.078 $\mu\text{mol kg}^{-1}$ for phosphate. Regional standard
195 deviation of nitrate measurements below 1000 db varied between 0.08 $\mu\text{mol kg}^{-1}$ in the Gulf of Lion
196 (DF2) with cruise #9 and 1.6 $\mu\text{mol kg}^{-1}$ in the Balearic Sea (DS2) observations of cruise #14.
197 Phosphate lowest regional standard deviation was 0.01 $\mu\text{mol kg}^{-1}$ found in the observations of cruise
198 #9 in Gulf of Lion (DF2), cruise #10 in Balearic Sea (DS2) and Algerian West (DS3), cruise #14 and

199 cruise # 15 in Tyrrhenian South (DT3), cruise #18 in Algero-Provençal (DF1) and Sardinia Channel
200 (DI1) while the highest standard deviation was $0.1 \mu\text{mol kg}^{-1}$ in the observations of cruise #12 in
201 Algerian West (DS3). As for silicate, the lowest standard deviation was $0.02 \mu\text{mol kg}^{-1}$ observed in
202 cruise #9 measurements of Gulf of Lion subregion (DF2) and the highest deep standard deviation was
203 observed in cruise #6 in its all subregions together with cruise #5 measurement in Tyrrhenian North
204 (DT1) with $1.83 \mu\text{mol kg}^{-1}$ standard deviation.

205 Cruises #3, #6 and #9 had the largest spatial extension (see right side of Fig. 9) with a high number of
206 samples over more than seven subregions (Table 4), the geographical variability of the distribution in
207 dissolved inorganic nutrients results thus in the largest standard deviations. Conversely, cruises with
208 smaller spatial coverages have lower standard deviations. Therefore, a relatively small spatial
209 coverage and high standard deviation is considered as indicative of data with low precision (Olsen et
210 al., 2016). This applies to cruises #1, #5, and #16. Despite the small spatial coverage, samples of
211 nitrate and phosphate of cruise #5 have an overall standard deviation of $1.35 \mu\text{mol kg}^{-1}$ and $0.07 \mu\text{mol}$
212 kg^{-1} , respectively, a high standard deviation pointed out also in the regional standard deviation of deep
213 measurements in Tyrrhenian North (DT1) and South (DT3) . Cruise #1, with few stations in
214 Tyrrhenian North (DT1) and South (DT3) subregions and 21 samples below 1000 db, has an overall
215 standard deviation of $1.25 \mu\text{mol kg}^{-1}$ for nitrate, $0.06 \mu\text{mol kg}^{-1}$ for phosphate and $1.64 \mu\text{mol kg}^{-1}$ for
216 silicate. The regional standard deviation was relatively high for nitrate ($0.51\text{-}1.32\mu\text{mol kg}^{-1}$),
217 phosphate ($0.02\text{-}0.065\mu\text{mol kg}^{-1}$) and silicate ($0.53\text{-}1.83\mu\text{mol kg}^{-1}$). A comparison with the deviations
218 from e.g. cruise # 2, carried out in the same year and e.g. cruise #17 (with a similar cruise track),
219 confirms the lower precision of the data of cruise #1. Similar considerations apply to the quality of
220 nitrate samples ($0.87\text{-}1.02 \mu\text{mol kg}^{-1}$) and silicate ($0.87\text{-}0.9 \mu\text{mol kg}^{-1}$) from cruise #16, covering a
221 small area in Tyrrhenian North (DT1) and South (DT3), compared to cruise #17, carried out in the
222 same regions (right side of Fig. 9 and Table 4).

223 Deep silicate measurements of cruise #6 have twice the overall standard deviation of silicate data of
224 cruise #8 from the same year. Adding to that, in the seven subregions, the regional standard deviation
225 of deep silicate observations was the highest, between 1.04-2 $\mu\text{mol kg}^{-1}$ which was relatively high
226 compared to the surrounding cruises that have observations in the same subregions. This is again
227 suggestive of the limited precision. On the other hand, trying to explain the source of relatively high
228 standard deviations in specific cruises is not always straightforward, as they could stem from a variety
229 of sources, sampling, conservation and analysis. The bottom water in the WMED exhibits a high
230 nutrient content below 1000 db (Table 4), due to the longer residence time. Dividing the WMED into
231 subregions, has effectively removed the natural spatial change in nutrients, making the interpretation
232 of the standard deviation a matter of the precision of the measurements only.

233 In Table 4, deep averages by subregions showed that overall nutrient concentration fluctuated around
234 $7.4 \pm 0.9 \mu\text{mol kg}^{-1}$ for nitrate, $0.3 \pm 0.06 \mu\text{mol kg}^{-1}$ for phosphate and $7.7 \pm 0.8 \mu\text{mol kg}^{-1}$ for silicate,
235 similar findings were reported by Manca et al. (2004). Comparing cruise averages in each region
236 enabled the identification of “suspect” cruises. Cruise #24 has the lowest deep average in nitrate in
237 Algero-Provençal (DF1), Tyrrhenian North (DT1) subregions and Sardinia Channel (DI1). As for
238 silicate of cruises #24 and #16 was very low compared to the overall regional average in Liguro-
239 Provençal (DF3) and Tyrrhenian South (DT3) subregions. Deep average of phosphate did not show
240 any outlier cruises in all subregions. Different reasons could explain the low precision in the samples,
241 freezing is one. Although it is a valid preservation method (Dore et al., 1996), the error is higher when
242 samples were not analysed immediately (Segura-Noguera et al., 2011), so the storage time could
243 influence.

244 **3.2 Secondary Quality control: the crossover analysis**

245 The method used to perform the secondary QC on the WMED dissolved inorganic nutrient dataset
246 makes use of the quality-controlled reference data, and the crossover analysis toolbox developed by
247 Tanhua (2010a) and Lauvset and Tanhua (2015). The computational approach is based on comparing

248 the cruise data set to a high-quality reference data set to quantify biases, described in detail in Tanhua
249 et al. (2010b). Here, we summarize the technique with emphasis on inorganic nutrients. The first step
250 consisted of selecting reference data, as described in section 2.3. The second step is the crossover
251 analysis that was carried out using a MATLAB Toolbox (available online: [https://cdiac.ess-
253 dive.lbl.gov/ftp/oceans/2nd_QC_Tool_V2/](https://cdiac.ess-
252 dive.lbl.gov/ftp/oceans/2nd_QC_Tool_V2/)) where crossovers are generated as difference between two
254 cruises using the “running cluster” crossover routine. Each cruise is thus compared to the chosen set of
255 reference cruises. For each crossover, samples deeper than 1000 db are selected within a predefined
256 maximum distance set to 2°arc distance, defined as a crossing region, to ensure the quality of the
257 offset with a minimum number of crossovers and to minimize the effect of the spatial change. The
258 reason to select measurements deeper than 1000 db, is to remove the high frequency variability
259 associated to mesoscale features, biological activity and the atmospheric forcing acting in the upper
260 layers, that might induce changes in biogeochemical properties of water masses. On the other hand,
261 also the deep Mediterranean cannot be considered truly “unaffected” by changes, as it is intermittently
262 subjected to ventilation (Schroeder et al., 2016; Testor et al., 2018) and the real variability can be
263 altered in adjusting data. The computational approach takes this into account, since weights are given
264 to the less variant profile in the crossing region, according to the “confidence” in the determined offset
265 of the compared profiles (i.e. the weighted mean offset of a given crossover-pair is weighted to the
266 depth where the offsets of all compared profiles have the smallest variation which indeed is strongly
267 interlinked with the degree of variance of each profile) (for further details see Lauvset and Tanhua,
2015).

268 Before identifying crossovers, each profile was interpolated using the piecewise cubic Hermite method
269 and the distance criteria outlined in Lauvset and Tanhua (2015), their Table 1a, detailed in Key et al.
270 (2004). The crossover is a comparison between each interpolated profile of the cruise being evaluated
271 and the interpolated profile of the reference cruise. The result is a weighted offset (defined as
272 difference cruise/reference) and a standard deviation of the offset. The standard deviation is indicative

273 of the precision; however, it is important to note that this assumption only works because it is a
274 comparison to a reference, and the absolute offset is indicative of accuracy.

275 The third step consists in evaluating and selecting the suggested correction factor that was applied to
276 the whole water column. The correction factor was calculated from the weighted mean offset of all
277 crossovers found between the cruise and the reference data set, involving a somewhat subjective
278 process.

279 For inorganic nutrients, offsets are multiplicative so that a weighted mean offset > 1 means that the
280 measurements of the corresponding cruise are higher than the measurements of the reference cruise in
281 the crossing region and applying the adjustment would decrease the measured values. The magnitude
282 of an increase or a decrease is the difference of the weighted offset from 1. In general, no adjustment
283 smaller than 2% (accuracy limit for nutrient measurements) is applied (detailed description is found in
284 Hoppema et al., 2009; Lauvset and Tanhua, 2015; Olsen et al., 2016; Sabine et al., 2010; Tanhua et al.,
285 2010b).

286 The last step is the computation of the weighted mean (WM) to determine the internal consistency and
287 quantify the overall accuracy of the adjusted product (Hoppema et al., 2009; Sabine et al., 2010;
288 Tanhua et al., 2009), with the difference that our assessment is based on the offsets with respect to a
289 set of reference cruises. This WM reflects the absolute weighted mean offset of the data set compared
290 to the reference data set, hence the smaller the WM the higher the internal consistency. The accuracy
291 was computed from the individual absolute weighted offsets. The WM, which will be discussed in
292 section 4.4., was computed using the individual weighted absolute offset (D) of number of crossovers

293 (L) and the standard deviation (σ): $WM = \frac{\sum_{i=1}^L D(i)/(\sigma(i))^2}{\sum_{i=1}^L 1/(\sigma(i))^2}$

294 **4 Results of the secondary QC and recommendations**

295 The results of the secondary QC revealed the necessary corrections for nitrate, phosphate and silicate.
296 Four cruises were not considered in the crossover analysis: cruises #7 and #11 do not have enough
297 stations > 1000 db (at least 3 to get valid statistics), while cruises #19 and #21 were outside the spatial
298 coverage of the reference cruises. Cruises that were not used for the crossover analysis are made
299 available in the original dataset but were not included in the final data product (see Supplementary
300 material – Part 2 (A2)).

301 Overall, we found a total number of 73 individual crossovers for nitrate, 72 for phosphate and 54 for
302 silicate. An example of the running cluster crossover output is shown in Fig.4. Results of the crossover
303 analysis is an adjustment factor for each cruise and each nutrient, that are shown in Table 5 and Fig. 5-
304 6-7. The adjustment factor was calculated from the weighted mean of absolute offset summarized in
305 Table 6 and Fig. 3S-4S-5S. Table 6 details the improvement of the weighted mean of absolute offset
306 by cruise prior to and after adjustments, the information is also displayed graphically in Fig. 3S-4S-5S.
307 Cruises are in chronological order in all figures and tables.

308 **4.1 Nitrate**

309 The crossover analysis suggests a significant adjustment for nitrate concentrations on 15 cruises,
310 between 0.94 and 0.98 (for adjustments <1) and between 1.02 and 1.34 (for adjustments >1) (Table 5
311 and Fig.5). Offsets suggest that the deep measurements of cruises #1, #3, #4, #5, #6, #8, #12, #13, #15,
312 #16, #23 and #24 need to be adjusted towards higher concentrations, when compared to the respective
313 reference (Fig.3S).

314 Nitrate observations of cruises #2, #9 and #10 on the other hand were higher than the reference cruises
315 and exhibit variation outside the accepted accuracy limit, thus require a downward adjustment.

316 Finally, five cruises (#14, #17, #18, #20, and #22) were consistent with the reference data and no
317 adjustment was necessary. Considering the weighted mean of absolute offset after adjustments shown

318 in Table 6, two cruises (#5 and #24) required large correction factors but remain outside the accuracy
319 threshold (Fig. 5). These cruises are considered in detail later (section 4.4).

320 **4.2 Phosphate**

321 For phosphate the crossover analysis suggests adjustments for 20 cruises, as shown in Fig. 6. Deep
322 phosphate measurements of 15 cruises (Table 6) appear to be lower than the respective reference
323 measurements (i.e. phosphate data of these cruises require an upward adjustment), while the data of
324 five cruises (#2, #3, #4, #6, #24) are higher (i.e. they need a downward adjustment) (Fig.4S). Applying
325 all the indicated adjustments, the large offsets of cruises #2, #3, #4, #6, #8, #9, #10, #18, #20, #23 and
326 #24 are reduced and became consistent with the reference. Cruises #1, #5, #12, #13, #14, #15, #16,
327 #17, and #22 retain an offset even after applying the indicated adjustment. These cruises are
328 considered in detail later.

329 According to Olsen et al. (2016), if a temporal trend is detected in the offsets, no adjustments should
330 be applied. There is indeed a decreasing trend between 2008 and 2017 in the phosphate correction
331 factor (Fig. 6), and thus an increasing one in the weighted mean offset (Fig.4S), implying a temporal
332 increase of phosphate. Therefore, phosphate data of the cruises being part of the trend were not
333 flagged as questionable, except some cruises that are discussed further in section 4.4.

334 Comparing phosphate before and after adjustment, the corrections did minimise the difference with the
335 reference, while the actual variation with time was preserved (Fig.6). The temporal trend towards
336 higher phosphate concentrations in the Mediterranean Sea is considered to be real, even though
337 studies concerning the biogeochemical trends in the deep layers of the WMED are scarce (Pasqueron
338 et al., 2015). However, this variation could be consistent with the findings of Béthoux et al.(1998,
339 2002) and the modelling studies by Moon et al. (2016) and Powley et al. (2018) who indeed found an
340 increasing trend in phosphate concentrations over time, due to the increase in the atmospheric and
341 terrestrial inputs.

342 **4.3 Silicate**

343 The results of the crossover analysis for silicate suggests corrections for all cruises (Fig.7). The
344 crossovers indicate that deep silicate measurements are lower in the evaluated cruises than in the
345 corresponding reference cruises (i.e. they need to be adjusted upward) (Fig.5S). This is likely to be a
346 direct result of freezing the samples before analysis, since the reactive silica polymerizes when frozen
347 (Becker et al., 2019). After applying the adjustment (Table 5), as expected, the offsets are reduced
348 (Table 6), but five cruises (#1, #5, #6, #15, and #16) remain outside the accuracy envelope. Due to the
349 large offsets, these cruises will be discussed further in section 4.4.

350 **4.4 Discussion and recommendation**

351 Adjustments were evaluated for each cruise separately. As a general rule, no correction was applied
352 when the suggested adjustment is strictly within the 2% limit (indicated with NA in Table 5). The
353 average correction factors were 1.06 for nitrate, 1.14 for phosphate and 1.14 for silicate, respectively.
354 To verify the results, we re-ran the crossover analysis and re-computed offsets and adjustment factors
355 using the adjusted data (as shown in blue in Fig. 3S-4S-5S and Fig. 5-6-7). Most of the new
356 adjustments are within the accuracy envelope and few are outside the limit, except for the cruises
357 belonging to the above mentioned “phosphate-trend” and the other outlying cruises which are detailed
358 hereafter. By the application of adjustments, the deep-water offsets were reduced. This can be seen in
359 the decrease of the weighted mean offset between the data before adjustments (after 1st QC, Fig. 3S-
360 4S-5S, in grey) and the adjusted data (after 2nd QC, Fig. 3S-4S-5S, in blue).

361 Referring to the analysis detailed in section 3.2, the internal consistency of the nutrient data set has
362 improved and increased significantly after the adjustment, from 4% for nitrate, 19% for phosphate and
363 13% for silicate, to a more unified dataset with 3 % for nitrate, 6 % for phosphate and 3% for silicate.

364 A comparison between the original and the adjusted nutrient observations is shown in Fig. 8A-B-C,
365 indicating an improvement in the accuracy based on the reference data and a relatively reduced range

366 particularly for phosphate (Fig. 8B). Figure 8. D-E scatterplots show that after the quality control,
367 nutrient stoichiometry slopes obtained from regressions, between tracers along the water column
368 demonstrate a strong coupling and provide a nitrate to phosphate ratio of ~ 22.09 and a nitrate to
369 silicate ratio of ~ 0.94 . These values are consistent with nutrient ratios range found in the WMED as
370 reported in Lazzari et al. (2016); Pujo-Pay et al., (2011) and Segura-Noguera et al. (2016). The
371 regression model is more accurate after adjustments with an improved r^2 for N:P (from 0.81 to 0.90)
372 and for N: Si (from 0.85 to 0.87).

373

374 In the following some details on the adjustment of specific cruises are given:

375 Cruise #2 [48UR20041006] needed an adjustment of 0.98 for nitrate, 0.9 for phosphate and 1.06 for
376 silicate. Most of the crossover profiles occur in the Tyrrhenian Sea (Tyrrhenian North and Tyrrhenian
377 South subregions). After adjustment, the cruise is inside the 2% envelope.

378 Cruise #3 [48UR20050412] appeared to be outside the 2% envelope before adjustments. Its offsets
379 with five reference cruises, crossing the Tyrrhenian Sea, Sardinia Channel, Gulf of Lion and Algero-
380 Provençal subregions, showed that nitrate and silicate values to be relatively low, and thus an
381 adjustment of 1.08 and 1.15 was applied respectively. On the other hand, phosphate values were
382 relatively high, and a 0.93 adjustment was applied.

383 Cruise #4 [48UR20050529] correction factor estimate was based on five crossovers that covered five
384 subregions: Tyrrhenian South, Sardinian Channel, Algerian East and West and the Alboran Sea. Table
385 4 show that there are no large differences between regional averages within the cruise which justify an
386 adjustment of 1.04 for nitrate, 0.85 for phosphate and 1.183 for silicate.

387 Cruise #8 [48UR20060928] was adjusted by 1.03 for nitrate, 1.14 for phosphate and 1.1 for silicate,
388 because it showed values to be low compared to four references. After adjustment, the data were
389 inside the acceptable range.

390 Cruise #9 [48UR20071005] values of nitrate were slightly outside the 2% envelope before
391 adjustments, similar to phosphate and silicate that were lower compared to the reference. The
392 adjustments of 0.97 for nitrate, 1.14 for phosphate and 1.115 for silicate suggested by the mean offset
393 against the reference cruises were recommended.

394 Cruise #13 [48UR20090508] has three crossovers in the common crossing zone that included
395 Tyrrhenian North, Tyrrhenian South and Sardinia Channel subregions. The crossover suggests that this
396 cruise has too low values and needs an adjustment of 1.05 for nitrate, 1.33 for phosphate and 1.15 for
397 silicate.

398 Cruise #14 [48UR20100430] has a mean offset with four reference cruises that suggests an adjustment
399 factor of 1.34 for phosphate and 1.123 for silicate. Nitrate did fall within the accuracy envelope; no
400 adjustment was needed.

401 Cruise #10 [48UR20080318] has only three crossovers in the Algero-Provençal subregion, showing
402 that nitrate is too high compared to the reference while phosphate and silicate are slightly lower. We
403 therefore applied the adjustments of Table 5, since the deep averages in each region (Table 4) did not
404 show large regional difference.

405 Cruise #17 [48UR20110421] crossover analysis did not suggest any correction for nitrate; however,
406 with an offset based on two crossovers in the Tyrrhenian North and South subregions, adjustments
407 were recommended for phosphate (1.25) and silicate (1.12), for being lower than the reference cruises.

408 Cruise #18 [48UR20111109] is similar to cruise #17, since it was suggested to adjust phosphate by
409 1.14 and silicate by 1.09, based on four crossovers in the Tyrrhenian North and South, Sardinia
410 Channel and Algero-Provençal subregions.

411 Cruise #20 [48UR20120111] has four crossovers over the Tyrrhenian North and South and Algero-
412 Provençal subregions. Its measurements were slightly lower than the reference cruises suggesting a
413 correction factor of 1.17 for phosphate and 1.08 for silicate.

414 Cruise #22 [48UR20131015] has similar correction factors as cruise #20, based on three crossovers in
415 the Sardinia Channel and Tyrrhenian North and South subregion, with measurements being lower than
416 the reference.

417 Cruise #23 [48QL20150804] showed nutrient values slightly lower than the reference cruises as well,
418 suggesting small correction factors of 1.02 for both nitrate and phosphate and 1.08 for silicate, a
419 correction factors that were based on offsets with five cruises.

420 Below, we discuss the recommended flags in the final product (Table 3; see supplementary Materials
421 Part-2 (A2)) assigned for some cruises that needed further consideration, since they required larger
422 adjustment factors:

423 Cruise #1 [48UR20040526]: The adjusted values are still lower than the reference (Fig.5-6-7-Fig.3S-
424 4S-5S) and are still outside the 2% accuracy range. This cruise had stations in the Sicily Strait,
425 Tyrrhenian North and South and Ligurian East subregions (Fig. 9, right side) and only 4 stations were
426 deeper than 1000 db (those within the Tyrrhenian Sea). The low precision of this cruise has already
427 been evidenced during the 1st QC (section 3.1). We recommend flagging this cruise as questionable
428 (flag 3).

429 Cruise #5 [48UR20051116]: This cruise took place between Sicily Strait and the Tyrrhenian North and
430 South (Fig. 9, right side). Nitrate, phosphate and silicate data were lower than those from other cruises

431 (#3 and #4) run the same year (Fig. 5-6-7-Fig.3S-4S-5S) and are still biased after adjustments.
432 Considering the limited precision and the low number of crossovers, it is recommended to flag the
433 cruise as questionable (flag 3).

434 Cruise #6 [48UR20060608]: This cruise had an offset with five cruises giving evidence that
435 adjustments of 1.05 for nitrate, 0.86 for phosphate and 1.26 for silicate are needed. The silicate bias
436 was reduced after adjustment but remained large with respect to the accuracy limit (Fig. 7-Fig. 5S).
437 This cruise has a wide geographic coverage, with stations along 9 sections (Fig. 9, right side).
438 Considering also the high standard deviation (Table 4), which is partially attributed to the spatial
439 coverage of the cruise, there is still uncertainty about the quality of the samples. It is recommended to
440 flag silicate data of cruise #6 as questionable (flag 3).

441 Cruise #12 [48UR20081103]: Phosphate data have low accuracy with respect to the reference cruises
442 (Fig. 6-Fig. 4S). This cruise has stations along a longitudinal section from Sicily Strait to the Alboran
443 Sea, which might explain the large standard deviation of deep phosphate samples (Table 4). Cruise
444 #12 was given a correction of 1.08 for nitrate, 1.12 for silicate and 1.38 for phosphate. The mean
445 offset from five crossovers computed within the Tyrrhenian South, Sardinia Channel, Algerian East,
446 Algerian West and Alboran Sea subregions suggests that this cruise has lower nutrient values than the
447 reference cruise. After adjustment, cruise #12 is within the acceptable range for nitrate and silicate but
448 not for phosphate as highlighted in section 3.2. In addition, considering the relatively high number of
449 stations >1000 db and a plausible trend in phosphate, it is recommended to flag the phosphate data as
450 good/acceptable (flag 2).

451 Cruise #15 [48UR20100731]: This cruise has 149 station along a similar track as cruise #12 but shows
452 larger offsets for phosphate and silicate (Fig. 6-7-Fig. 4S-5S), compared to cruise #12. Considering
453 that deep silicate data was not of low quality (small standard deviation, see Table 4), and that deep
454 phosphate fall within the “phosphate-trend” discussed above, these data are flagged good/acceptable
455 (flag 2).

456 Cruise #16 [48UR20101123]: The cruise shows large offsets for phosphate and silicate (Fig. 6-7- Fig.
457 4S-5S), similar to cruise #15. Considering that the overall cruise standard deviation of silicate samples
458 below 1000 db was relatively high (1.02 over 14 samples, see Table 4), and that it has only one
459 crossover between the Tyrrhenian North and South subregions (Table 6), and that when comparing
460 deep regional averages, this cruise had the lowest average silicate value, it is recommended to flag
461 silicate data of cruise #16 as questionable (flag 3). As for phosphate, the cruise is part of the
462 “phosphate-trend” and is therefore flagged good/acceptable (flag 2).

463 Cruise #24 [48QL20171023]: This cruise has the largest offset for nitrate even after adjustment. It is
464 very likely due to a difference between laboratories (calibration standards) concerning nitrate, which
465 needs to be flagged as questionable (flag 3) in the final product.

466 There are several sources of bias in the observation. One of the main reasons for an upward/
467 downward bias would be the difference in the nutrient’s chemical analytical method and the lack of
468 use of CRM in all cruises as also noted in CARINA (Tanhua et al., 2009) or in the most recent global
469 comparability study by Aoyama (2020).

470 Cruises discussed in this section were not removed from the final product but are retained along with
471 their recommended quality flag (Table 3) detailed above and in the supplementary material – Part 2
472 (A2)). We have done the evaluation of their overall quality but leave it up to the users how to
473 appropriately use these data.

474 **4.5 Product assessment: Comparison with MEDATLAS**

475 Averages water mass biogeochemical properties have been computed from the adjusted product (Table
476 7), and compared to the MEDAR/Medatlas annual climatological profiles, downloaded from the
477 Italian NODC website (<http://doga.ogs.trieste.it/medar/>) given by Manca et al. (2004), in order to
478 evaluate and asses the new product. Since nutrient properties exhibit differences with depths, we

479 compared average nutrient concentrations of the three main water masses in twelve subregions of the
480 WMED (Table 7, Fig 2S).

481 The results of Table 7 compares water mass biogeochemical properties with the reference climatology.
482 The new product agrees well with the Medatlas climatology. However, there are some distinctions.
483 The surface layer (0-150db) is characterized by a low nutrient content. The surface nitrate varies
484 between 0.69 and 2.75 $\mu\text{mol kg}^{-1}$ with a maximum found in the Ligurian East (DF4) and the minimum
485 in the Alboran Sea (DS1) subregions, similar values were recorded in the climatology (0.61- 3.00
486 $\mu\text{mol kg}^{-1}$). The differences in nitrate averages in the surface layer are observed in the Gulf of Lion
487 (DF2) where the new product is higher than the climatology and slightly lower in the Liguro-
488 Provençal (DF3). As for, the surface content in phosphate, it varied between 0.04 and 0.16 $\mu\text{mol kg}^{-1}$
489 with a maximum found in the Ligurian East (DF1) and a minimum in the Alboran Sea (DS1), alike the
490 Medatlas climatology, where phosphate averages fluctuate between 0.05 and 0.19 $\mu\text{mol kg}^{-1}$. The new
491 product is slightly lower compared to the climatology. As to the average surface in silicate, it varies
492 between 1.36 and 2.91 $\mu\text{mol kg}^{-1}$ with a minimum found in the Ligurian East (DF4), the maximum in
493 the Gulf of Lion (DF2)) while in the climatology, it varied between 1.27 and 2.31 $\mu\text{mol kg}^{-1}$ (the
494 minimum in the Ligurian East (DF4) and the maximum in the Alboran Sea (DS1)). The new product is
495 slightly higher in silicate.

496 Overall, the differences in the surface layer are observed in the Gulf of Lion (DF2), the Liguro-
497 Provençal (DF3) and the Ligurian East (DF4) regions which could be due to the intense variability of
498 the vertical mixing occurring in the northern WMED compared to the other subregions.

499 In the intermediate layer, averages were computed from the depth of the salinity maximum (S_{max})
500 $\pm 100\text{m}$ from a regional average profile, indicative of the Levantine Intermediate Water (LIW) core.
501 Nitrate average varied between 4.94 and 9.32 $\mu\text{mol kg}^{-1}$ where the minimum content was recorded in
502 Sicily strait (DI3) and the maximum in the Algerian West (DS3) while in the Medatlas climatology,
503 nitrate was between 5.14 and 8.60 $\mu\text{mol kg}^{-1}$. In average, the lowest content in nitrate was in the

504 Tyrrhenian North (DT1) and South (DT3), Sardinia Channel (DI1) and Sicily Strait (DI3) while LIW
505 of the Gulf of Lion (DF2), Liguro-Provençal (DF3), Ligurian East (DF4), Balearic Sea (DS2), Algero-
506 Provençal (DF1), Alboran Sea (DS1), Algerian West (DS3) and East (DS4) subregions was relatively
507 rich in nitrate. Compared to the Medatlas product, though the new product was slightly higher mainly
508 in the Gulf of Lion (DF2), Ligurian East (DF4) and Balearic Sea (DS2). As for phosphate, LIW
509 averages showed similar behavior as nitrate, the lowest phosphate content ($0.21-0.27 \mu\text{mol kg}^{-1}$) was
510 observed in the Eastern subregions of WMED (DI3, DI1, DT3 and DT1), when the maximum
511 concentrations ($0.4-0.37 \mu\text{mol kg}^{-1}$) were reported in the Western subregions of the WMED (DS1, DS3
512 and DS4, DS2 and DF2). The large differences between the two products were in the Ligurian East
513 (DF4) and the Alboran Sea (DS1), subregions of few numbers of observations.

514 Concerning silicate, the lowest average concentration ($5.25 \mu\text{mol kg}^{-1}$) was observed in LIW core of
515 Sicily Strait (DI3,) and the maximum concentrations ($8.66 - 8.77 \mu\text{mol kg}^{-1}$) were in the Alboran Sea
516 (DS1) and Gulf of Lion (DF2), similar values were recorded in the Medatlas climatology ($4.86-7.95$
517 $\mu\text{mol kg}^{-1}$). There are some discrepancies, where the new product was higher particularly in the Gulf
518 of Lion (DF2), Liguro-Provençal (DF3) and Algerian West (DS3) subregions. This difference is
519 explained by the limited number of observations within depth range in the new product compared to
520 the observations used in the climatology in these subregions.

521 Referring to Manca et al.,(2004), the LIW core salinity values are relatively more pronounced in Sicily
522 Strait (DI3), Sardinia Channel (DI1) and in the Tyrrhenian South (DT3) and North (DT1) subregions,
523 where nutrients were lower than the Western subregions (DS3, DS4, DS1, DF1, DS2, DF4, DF3,
524 DF2). The averages of nutrient within the LIW core ties well with the Medatlas climatology averages
525 (Table 7), except in subregions with important vertical mixing.

526 We have verified also average biochemical properties in the deep layer (below 1500db). The new
527 product is slightly higher in nitrate averages ($7.74 - 8.37 \mu\text{mol kg}^{-1}$) than the Medatlas climatology
528 ($7.12 - 8.06 \mu\text{mol kg}^{-1}$) (Table 7). The largest difference was found in Tyrrhenian South (DT3) and

529 North (DT1) subregions. This difference could be due to the fact that, we are comparing two different
530 time periods (2004-2017 and 1908-2001). As for the deep layer phosphate, average concentrations
531 varied between 0.35 and 0.37 $\mu\text{mol kg}^{-1}$ and were within the climatology limits (0.31 - 0.40 $\mu\text{mol kg}^{-1}$).
532 In all subregions, there was not large differences. Overall, phosphate was in accordance with the
533 Medatlas climatology. Similar to nitrate, deep average silicate in the new product (8.64 -9.21 $\mu\text{mol kg}^{-1}$)
534 was higher than the climatology (7.51 to 9.04 $\mu\text{mol kg}^{-1}$). The largest difference in average silicate
535 was observed in the Tyrrhenian North (DT1), South (DT3) and Liguro-Provençal (DF3) subregions.

536 We then used the Root Mean Squared Error (RMSE) as statistical index to quantify the difference
537 between averaged regional profiles from the new product and Medatlas product. The climatology
538 annual profiles were interpolated to the regional average profiles of the new product, and the average
539 RMSE for each layer and subregion was calculated. Fig. 10 shows the regional evolution of RMSE in
540 the main water masses for the three nutrients. For nitrate (Fig. 10 A), the RMSE in the surface layer
541 varied between 0.12 $\mu\text{mol kg}^{-1}$ (in the Tyrrhenian North (DT1)) and 1.36 $\mu\text{mol kg}^{-1}$ (in the Gulf of
542 Lion (DF2)); in the intermediate layer, the RMSE was between 0.07 $\mu\text{mol kg}^{-1}$ (in the Sardinia
543 Channel (DI1)) and 2.35 $\mu\text{mol kg}^{-1}$ (in the Gulf of Lion (DF2)), and was lower in the deep layer,
544 between 0.11 $\mu\text{mol kg}^{-1}$ (in the Algerian East (DS4)) and 0.79 $\mu\text{mol kg}^{-1}$ (the Gulf of Lion (DF2)). The
545 RMSE decreases in the Algerian East (DS4), Tyrrhenian North (DT1), Tyrrhenian South (DT3),
546 Sardinia Channel (DI1) and Sicily Strait (DI3). This illustrates the low difference between the two
547 products.

548 For phosphate (Fig. 10 B), the RMSE ranges between 0.0022 $\mu\text{mol kg}^{-1}$ (in the Tyrrhenian South
549 (DT3)) and 0.12 $\mu\text{mol kg}^{-1}$ (in the Ligurian East (DF4)) in the surface layer; and is between 0.003
550 $\mu\text{mol kg}^{-1}$ (in the Liguro-Provençal subregion (DF3)) and 0.048 $\mu\text{mol kg}^{-1}$ (in the Alboran Sea (DS1))
551 at intermediate depths, while in the deep layer RMSE varied between 0.0087 (in the Gulf of Lion
552 (DF2)) and 0.057 $\mu\text{mol kg}^{-1}$ (in the Tyrrhenian North (DT1)).

553 Regarding silicate RMSE (Fig. 10 C) in surface, it varied between $0.13 \mu\text{mol kg}^{-1}$ (in the Algero-
554 Provençal subregion (DF1)) and $3.5 \mu\text{mol kg}^{-1}$ (in the Ligurian East subregion (DF4)), A lower RMSE
555 between $0.10 \mu\text{mol kg}^{-1}$ (in the Sardinia Channel (DI1)) and $2.54 \mu\text{mol kg}^{-1}$ (in the Gulf of Lion (DF2))
556 was reported in the intermediate layer; the results in deep layer, were between $0.33 \mu\text{mol kg}^{-1}$ (in the
557 Algerian East (DS4)) and $1.43 \mu\text{mol kg}^{-1}$ (in the Liguro-Provençal subregion (DF3)).

558 The best agreement between the two products was observed in the intermediate and deep layer. The
559 lowest RMSE was confined to the deep layer in most of the subregions while the highest difference
560 was found in the surface layer since it is subjected to intense vertical mixing mainly in the northern
561 WMED. Comparing averages in subregions, showed similar differences in nutrient between the two
562 products particularly in the Gulf of Lion (DF2), the Liguro-Provençal (DF3), Ligurian East (DF4) and
563 Algerian East (DS4), due to the relative high variability in nutrient concentrations in these subregions.
564 These differences are not significant as there is discrepancy on the number of observations used in the
565 two products. Overall, inorganic nutrients of the new product agree very well with the
566 MEDAR/Medatlas climatology. The main features of the spatial distribution in the inorganic nutrients
567 were in accordance with the findings of Manca et al., (2004), where the relative high content in
568 nutrient was found in the intermediate layer of the Algerian subregions (DF1, DS3, DS4) than in other
569 subregions (Table 7). Besides, the highest concentrations in deep layer silicate were reported in the
570 Algerian subregions in the two products ($9.21 \mu\text{mol kg}^{-1}$ (DS3) in the new product; $9.04 \mu\text{mol kg}^{-1}$
571 (DS4) in the climatology), which is indicative of the poor regional ventilation and of the longer
572 residence time of deep water especially in these subregions.

573 **5 Final remarks**

574 An internally consistent data set of dissolved inorganic nutrients has been generated for the WMED
575 (2004-2017). The accuracy envelope for nitrate and silicate was set to 2%, a predefined limit used in
576 GLODAP and CARINA data products. Regarding phosphate data, these were almost entirely outside
577 this limit, because of its natural variations and the overall very low concentrations in the WMED, a

578 highly P-limited basin. Using a crossover analysis (2nd QC toolbox) to compare cruises with respect to
579 reliable reference data, improved the accuracy of the measurements by bias-minimizing the individual
580 cruises. The new product was broadly in consistent with the earlier climatology MEDAR/Medatlas.

581 The publication of a quality-controlled extensive (spatially and temporally) database of inorganic
582 nutrients in the WMED was timely and fills a gap in information that prevented baseline assessments
583 on spatial and temporal variability of biogeochemical tracers in the Mediterranean. In combination
584 with older databases in the same region (e.g. bottle data available in the MEDAR/Medatlas database),
585 this new data producte will thus constitute a pillar on which the Mediterranean marine scientific
586 community will be able to build on original research topics on biogeochemical fluxes and cycles and
587 their relation to hydrological changes that occurred in the period covered by the dataset. The dataset is
588 also relevant for the modelling community as it can be used as an independent data product to assess
589 reanalysis products or it can be assimilated in new reanalysis products.

590 **6 Data availability**

591 The final product is available as a .csv merged file from PANGAEA, and can be accessed at
592 <https://doi.pangaea.de/10.1594/PANGAEA.904172> (Belgacem et al. 2019).

593 Ancillary information is in the supplementary materials with the list of variables included in the
594 original and final product. Table 1a and Table 1b summarizes all cruises included in the dataset. The
595 dataset include frequently measured stations and key transects of the WMED with in situ physical and
596 chemical oceanographic observations. As mentioned, two files are accessible, both include
597 oceanographic variables observed at the standard depths (see supplementary Materials Part-2).

598 - *Original dataset: CNR_DIN_WMED_20042017_original.csv*: This is the original dataset with
599 flag variable for each of the following parameter: CTD salinity, nitrate, phosphate and silicate
600 from the primary quality control (detailed in section 3.1).

601 - *Adjusted dataset: CNR_DIN_WMED_20042017_adjusted.csv*: This is the product after
602 primary quality control and after applying the adjustment factors from the secondary quality
603 control. Recommendations of section 4.4 are included, as well as quality flags.

604 **Author contribution:** MB, MA, SL, JC and KS substantially contributed to write the manuscript. SC,
605 GC and FA run the chemical analysis and contributed to the manuscript. MB coordinated the technical
606 aspects of most of the cruises. SC, GC, FA, AR, BP contributed in specific part of the manuscript.

607 **Acknowledgements.** The data have been collected in the framework of several of national and
608 European projects, e.g.: KM3NeT, EU GA #011937; SESAME, EU GA #GOCE-036949; PERSEUS,
609 EU GA #287600; OCEAN-CERTAIN, EU GA #603773; COMMON SENSE, EU GA #228344;
610 EU FLEETS, EU GA #228344; EU FLEETS2, EU GA # 312762; JERICO, EU GA #262584;
611 the Italian PRIN 2007 program “Tyrrhenian Seamounts ecosystems”, and the Italian RITMARE
612 Flagship Project, both funded by the Italian Ministry of University and Research. We thank Sarah
613 Jutterström from the Swedish Environmental Research institute for the invaluable help in Quality
614 Control discussions. We would like to express our appreciation to the INOCEN laboratory team at
615 IEO for their help and collaboration during MB’s stay there. The authors are deeply indebted to all
616 investigators and analysts who contributed to data collection at sea during so many years, as well as to
617 the PIs of the cruises (S. Aliani, M. Astraldi, M. Azzaro, M. Dibitto, G. P. Gasparini, A. Griffa, J.
618 Haun, L. Jullion, G. La Spada, E. Manini, A. Perilli, C. Santinelli, S. Sparnocchia), the captains and
619 the crews for allowing the collection of this enormous dataset; without them, this work would not have
620 been possible.

621

622

623

624
625
626
627
628
629
630
631
632
633
634
635
636
637

638 **References** Aoyama, M., Woodward, E., Malcolm, S., Bakker, K., Becker, S., Björkman, K., Daniel,
639 A., Mahaffey, C., Murata, A., Naik, H., Tanhua, T., Rho, T., Roman, R. and Sloyan, B.: Comparability
640 of oceanic nutrient data, Poster Cluster Community Whitepaper, CLIVAR Open Science Conference
641 on "Charting the course for climate and ocean research", 18-25 September 2016, Qingdao (China), 12
642 pp., <http://hdl.handle.net/10261/17137>, 2016.

643 Aoyama, M.: Global certified-reference-material-or reference-material-scaled nutrient gridded dataset
644 GND13. Earth System Science Data, 12, 487-499, <https://doi.org/10.5194/essd-12-487-2020>, 2020.

645 Becker, S., Aoyama, M., Woodward, E.M.S., Bakker, K., Coverly, S., Mahaffey, C., and Tanhua, T.:
646 GO-SHIP Repeat Hydrography Nutrient Manual: The precise and accurate determination of dissolved

647 inorganic nutrients in seawater, using Continuous Flow Analysis methods, In: The GO-SHIP Repeat
648 Hydrography Manual: A Collection of Expert Reports and Guidelines, 56 ,
649 <http://dx.doi.org/10.25607/OBP-555>, 2019.

650

651 Belgacem, M., Chiggiato, J., Borghini, M., Pavoni, B., Cerrati, G., Acri, F; Cozzi, S., Ribotti, A.,
652 Álvarez, M., Lauvset, S. K., Schroeder, K.: Quality controlled dataset of dissolved inorganic nutrients
653 in the western Mediterranean Sea (2004-2017) from R/V oceanographic cruises. PANGAEA,
654 <https://doi.pangaea.de/10.1594/PANGAEA.904172>, 2019.

655 Bethoux, J. P.: Oxygen consumption, new production, vertical advection and environmental evolution
656 in the Mediterranean Sea, Deep Sea Research, Part A, Oceanographic Research Papers, 36(5), 769–
657 781, doi:10.1016/0198-0149(89)90150-7, 1989.

658 Bethoux, J. P., Morin, P., Madec, C. and Gentili, B.: Phosphorus and nitrogen behaviour in the
659 Mediterranean Sea, Deep Sea Research, Part A, Oceanographic Research Paper, 39(9), 1641–1654,
660 doi:10.1016/0198-0149(92)90053-V, 1992.

661 Bethoux, J. P., Gentili, B., Morin, P., Nicolas, E., Pierre, C. and Ruiz-Pino, D.: The Mediterranean
662 Sea : a miniature ocean for climatic and environmental studies and a key for the climatic functioning of
663 the North Atlantic, Progress in Oceanography, 44, 131–146, 1999.

664 Béthoux, J. P., Morin, P., Chaumery, C., Connan, O., Gentili, B. and Ruiz-Pino, D.: Nutrients in the
665 Mediterranean Sea, mass balance and statistical analysis of concentrations with respect to
666 environmental change, Marine Chemistry , 63(1–2), 155–169, doi:10.1016/S0304-4203(98)00059-0,
667 1998.

668 Béthoux, J. P., Morin, P. and Ruiz-Pino, D. P.: Temporal trends in nutrient ratios: Chemical evidence
669 of Mediterranean ecosystem changes driven by human activity, Deep Sea Research Part II Topical
670 Studies in Oceanography, 49(11), 2007–2016, doi:10.1016/S0967-0645(02)00024-3, 2002.

671 Boyd, P. W.: Beyond ocean acidification, Nature Geoscience, 4(5), 273–274, doi:10.1038/ngeo1150,
672 2011.

673 Coppola, L., Raimbault, P., Mortier, L., and Testor, P.: Monitoring the environment in the
674 northwestern Mediterranean Sea, Eos, 100, <https://doi.org/10.1029/2019EO125951>, 2019.

675 Dickson, A. G., Afghan, J. D. and Anderson, G. C.: Reference materials for oceanic CO₂ analysis: A
676 method for the certification of total alkalinity, Marine Chemistry, 80(2–3), 185–197,
677 doi:10.1016/S0304-4203(02)00133-0, 2003.

678 Dore, J. E., Houlihan, T., Hebel, D. V., Tien, G., Tupas, L., Karl, D. M.: Freezing as a method of
679 sample preservation for the analysis of dissolved inorganic nutrients in seawater, Marine
680 Chemistry, 53(3-4), 173-185, 1996.

681 Fichaut, M., Garcia, M. J., Giorgetti, A., Iona, A., Kuznetsov, A., Rixen, M. and Group, M.:
682 MEDAR/MEDATLAS 2002: A Mediterranean and Black Sea database for operational oceanography,
683 Elsevier Oceanography Series, 69, 645–648, doi:10.1016/S0422-9894(03)80107-1, 2003.

684 Giorgetti, A., Partescano, E., Barth, A., Buga, L., Gatti, J., Giorgi, G., Iona A., Lipizer, M.,
685 Holdsworth, N., Larsen, M.M., Schaap, D., Vinci, M., Wenzer, M. :EMODnet Chemistry Spatial Data
686 Infrastructure for marine observations and related information. *Ocean & Coastal Management*, 166, 9-
687 17, 2018. Giorgi, F.: Climate change hot-spots, *Geophysical Research Letters*, 33(8), 1–4,
688 doi:10.1029/2006GL025734, 2006.

689 Gouretski, V. V. and Jancke, K.: Systematic errors as the cause for an apparent deep water property
690 variability: Global analysis of the WOCE and historical hydrographic data, *Progress in Oceanography*,
691 48(4), 337–402, doi:10.1016/S0079-6611(00)00049-5, 2000.

692 Grasshoff, K., Kremling K., Ehrhardt M.: *Methods of seawater analysis* (3rd ed.), Weinheim
693 Press, WILEY-VCH, 203-273, 1999.

694 Hansen, H. P. and Koroleff, F.: Determination of nutrients, *Methods of Seawater Analysis*, 159–228,
695 1999.

696 Hoppema, M., Velo, A., van Heuven, S., Tanhua, T., Key, R. M., Lin, X., Bakker, D. C. E., Perez, F.
697 F., Ríos, A. F., Lo Monaco, C., Sabine, C. L., Álvarez, M. and Bellerby, R. G. J.: Consistency of
698 cruise data of the CARINA database in the Atlantic sector of the Southern Ocean, *Earth System*
699 *Science Data*, 1(1), 63–75, doi:10.5194/essd-1-63-2009, 2009.

700 Hydes, D. J., Aoyama, M., Aminot, A., Bakker, K., Becker, S., Coverly, S., Daniel, A., Dickson, A. G.,
701 Grosso, O., Kerouel, R., van Ooijen, J., Sato, K., Tanhua, T., Woodward, E. M. S. and Zhang, J. Z.
702 :Determination of Dissolved Nutrients (N, P, SI) in Seawater With High Precision and Inter-
703 Comparability Using Gas-Segmented Continuous Flow Analysers. In: *The GO-SHIP Repeat*
704 *Hydrography Manual: A Collection of Expert Reports and Guidelines. Version 1.* (eds Hood, E.M.,
705 C.L. Sabine, and B.M. Sloyan). IOCCP Report Number 14, ICPO Publication Series Number 134. 87
706 pp., <http://dx.doi.org/10.25607/OBP-555>, 2010.

707

708 Johnson, G. C., Robbins, P. E. and Hufford, G. E.: Systematic adjustments of hydrographic sections
709 for internal consistency, *Journal of Atmospheric Oceanic Technology*, 18(7), 1234–1244,
710 doi:10.1175/1520-0426(2001)018<1234:SAOHSF>2.0.CO;2, 2001.

711 Key, R. M., Kozyr, A., Sabine, C. L., Lee, K., Wanninkhof, R., Bullister, J. L., Feely, R. A., Millero,
712 F. J., Mordy, C. and Peng, T. H.: A global ocean carbon climatology: Results from Global Data
713 Analysis Project (GLODAP), *Global Biogeochem. Cycles*, 18(4), 1–23, doi:10.1029/2004GB002247,
714 2004.

715 Lauvset, S. K. and Tanhua, T.: A toolbox for secondary quality control on ocean chemistry and
716 hydrographic data, *Limnology and Oceanography Methods*, 13(11), 601–608,
717 doi:10.1002/lom3.10050, 2015.

718 Lazzari, P., Solidoro, C., Salon, S. and Bolzon, G.: Spatial variability of phosphate and nitrate in the
719 Mediterranean Sea: A modeling approach, *Deep Sea Research Part I*, 108, 39–52,
720 doi:10.1016/j.dsr.2015.12.006, 2016.

721 Lejeusne, C., Chevaldonné, P., Pergent-Martini, C., Boudouresque, C. F. and Pérez, T.: Climate
722 change effects on a miniature ocean: the highly diverse, highly impacted Mediterranean Sea, *Trends in*

723 Ecology and Evolution, 25(4), 250–260, doi:10.1016/j.tree.2009.10.009, 2010.

724 Manca, B., Burca, M., Giorgetti, A., Coatanoan, C., Garcia, M. J., and Iona, A. : Physical and
725 biochemical averaged vertical profiles in the Mediterranean regions: an important tool to trace the
726 climatology of water masses and to validate incoming data from operational oceanography. *Journal of*
727 *Marine Systems*, 48(1-4), 83-116, 2004.

728 Martín Míguez, B., Novellino, A., Vinci, M., Claus, S., Calewaert, J. B., Vallius, H., Schmitt, T.,
729 Pititto, P., Giorgetti, A., Askew, N., Iona, S., Schaap, D., Pinardi, N., Harpham, Q., Kater, B.J.,
730 Populus, J., She, J., Vasilev Palazov, A., McMeel, O., Oset, P., Lear, D., Manzella, G.M.R., Gorringer,
731 P., Simoncelli, S., Larkin, K., Holdsworth, N., Dimitrios_Arvanitidis C., Molina-Jack M.E., Chaves-
732 Montero M.D.M. , Herman, P.M.J., and Hernandez F.: The European marine observation and data
733 network (EMODnet): visions and roles of the gateway to marine data in Europe. *Frontiers in Marine*
734 *Science*, 6, 2019.

735 Moon, J., Lee, K., Tanhua, T., Kress, N. and Kim, I.: Temporal nutrient dynamics in the
736 Mediterranean Sea in response to anthropogenic inputs, , 5243–5251,
737 doi:10.1002/2016GL068788. Received, 2016.

738 Muniz, K., Cruzado, A., Ruiz De Villa, C. and Villa, C. R. De: Statistical analysis of nutrient data
739 quality (nitrate and phosphate), applied to useful predictor models in the northwestern Mediterranean
740 Sea, *Methodology*, 17, 221–231, 2001.

741 Olsen, A., Key, R. M., Heuven, S. Van, Lauvset, S. K., Velo, A., Lin, X., Schirnick, C., Kozyr, A.,
742 Tanhua, T., Hoppema, M. and Jutterström, S.: The Global Ocean Data Analysis Project version 2 (
743 GLODAPv2) – an internally consistent data product for the world ocean, , 297–323,
744 doi:10.5194/essd-8-297-2016, 2016.

745 Olsen, A., Lange, N., Key, R., Tanhua, T., Alvarez, M. et al.: GLODAPv2.2019 -an update of
746 GLODAPv2. *Earth Syst. Sci. Data*, 11 (3), pp.1437 - 1461. ff10.5194/essd-11-1437-2019ff. fhal-
747 02315662, 2019.

748 Pasqueron, O., Fommervault, D., Migon, C., Ortenzio, F. D., Ribera, M. and Coppola, L.: Temporal
749 variability of nutrient concentrations in the northwestern Mediterranean sea (DYFAMED time-series
750 station), *Deep. Res. Part I*, 100, 1–12, doi:10.1016/j.dsr.2015.02.006, 2015.

751 Powley, H. R., Krom, M. D. and Van Cappellen, P.: Phosphorus and nitrogen trajectories in the
752 Mediterranean Sea (1950–2030): Diagnosing basin-wide anthropogenic nutrient enrichment, *Progress*
753 *in Oceanography*, 162, 257–270, doi:10.1016/j.pocean.2018.03.003, 2018.

754 Pujo-Pay, M., Conan, P., Oriol, L., Cornet-Barthaux, V., Falco, C., Ghiglione, J. F., Goyet, C.,
755 Moutin, T. and Prieur, L.: Integrated survey of elemental stoichiometry (C, N, P) from the western to
756 eastern Mediterranean Sea, *Biogeosciences*, 8(4), 883–899, doi:10.5194/bg-8-883-2011, 2011.

757 Sabine, C. L., Hoppema, M., Key, R. M., Tilbrook, B., Van Heuven, S., Lo Monaco, C., Metzl, N.,
758 Ishii, M., Murata, A. and Musielewicz, S.: Assessing the internal consistency of the CARINA data
759 base in the Pacific sector of the Southern Ocean, *Earth System Science Data Discussions*, 2(2), 195–

760 204, doi:10.5194/essd-2-195-2010, 2010.

761 Schroeder, K., Tanhua, T., Bryden, H., Alvarez, M., Chiggiato, J. and Aracri, S.: Mediterranean Sea
762 Ship-based Hydrographic Investigations Program (Med-SHIP), *Oceanography*, 28(3), 12–15,
763 doi:10.5670/oceanog.2015.71, 2015.

764 Schroeder, K., Chiggiato, J., Bryden, H. L., Borghini, M. and Ben Ismail, S.: Abrupt climate shift in
765 the Western Mediterranean Sea, *Scientific Reports*, 1–7, doi:10.1038/srep23009, 2016. Segura-
766 Noguera, M., Cruzado, A. and Blasco, D.: The biogeochemistry of nutrients, dissolved oxygen and
767 chlorophyll a in the Catalan Sea (NW Mediterranean Sea), *Sci. Mar.*, 80(S1), 39–56,
768 doi:10.3989/scimar.04309.20a, 2016.

769 Segura-Noguera, M., Cruzado, A., & Blasco, D.: Nutrient preservation, analysis precision and quality
770 control of an oceanographic database of inorganic nutrients, dissolved oxygen and chlorophyll a from
771 the NW Mediterranean Sea. *Scientia Marina*, 75(2), 321-339, 2011.

772 Suzuki, T., Ishii, M., Aoyama, A., Christian, J. R., Enyo, K., Kawano, T., Key, R. M., Kosugi, N.,
773 Kozyr, A., Miller, L. A., Murata, A., Nakano, T., Ono, T., Saino, T., Sasaki, K., Sasano, D., Takatani,
774 Y., Wakita, M., and Sabine, C. L.: PACIFICA Data Synthesis Project, ORNL/CDIAC-159, NDP-092,
775 Carbon Dioxide Information Analysis Center, Oak Ridge National Laboratory, U. S. Department of
776 Energy, Oak Ridge, Tennessee, 2013.

777 Tanhua, T.: Hydrochemistry of water samples during MedSHIP cruise Talpro. PANGAEA,
778 <https://doi.org/10.1594/PANGAEA.902293>, 2019.

779 Tanhua, T.: Matlab Toolbox to Perform Secondary Quality Control (2nd QC) on Hydrographic Data,
780 ORNL CDIAC-158. Carbon Dioxide Inf. Anal. Center, Oak Ridge Natl. Lab. U.S. Dep. Energy, Oak
781 Ridge, Tennessee, 158, doi:10.3334/CDIAC/otg.CDIAC_158, 2010a.

782 Tanhua, T., Brown, P. J. and Key, R. M.: CARINA : Nutrient data in the Atlantic Ocean, *Earth
783 Science Data*, 1, 7–24, doi:10.3334/CDIAC/otg.CARINA.ATL.V1.0, 2009.

784 Tanhua, T., Heuven, S. van, Key, R. M., Velo, A., Olsen, A. and Schirnick, C.: Quality control
785 procedures and methods of the CARINA database, *Earth System Science Data*, 2, 35–49, 2010b.

786 Tanhua, T., Hainbucher, D., Schroeder, K., Cardin, V., Álvarez, M. and Civitarese, G.: The
787 Mediterranean Sea system: A review and an introduction to the special issue, *Ocean Science*, 9(5),
788 789–803, doi:10.5194/os-9-789-2013, 2013.

789 Testor, P., Bosse, A., Houpert, L., Margirier, F., Mortier, L., Legoff, H., Dausse, D., Labaste, M.,
790 Karstensen, J., Hayes, D., Olita, A., Ribotti, A., Schroeder, K., Chiggiato, J., Onken, R., Heslop, E.,
791 Mourre, B., D’ortenzio, F., Mayot, N., Lavigne, H., de Fommervault, O., Coppola, L., Prieur, L.,
792 Taillandier, V., Durrieu de Madron, X., Bourrin, F., Many, G., Damien, P., Estournel, C., Marsaleix,
793 P., Taupier-Letage, I., Raimbault, P., Waldman, R., Bouin, M. N., Giordani, H., Caniaux, G., Somot,
794 S., Ducrocq, V. and Conan, P.: Multiscale Observations of Deep Convection in the Northwestern
795 Mediterranean Sea During Winter 2012–2013 Using Multiple Platforms, *Journal of Geophysical
796 Research: Oceans*, 123(3), 1745–1776, doi:10.1002/2016JC012671, 2018.

797 Tintoré, J., Pinardi, N., Alvarez Fanjul, E., Balbin, R., Bozzano, R., Ferrarin, C.,... and Clementi, E.:
798 Challenges for Sustained Observing and Forecasting Systems in the Mediterranean Sea. *Frontiers in*
799 *Marine Science*, 6, 568, 2019.

800

801 **Figure Captions**

802 **Figure 1.** Map of the Western Mediterranean Sea showing the biogeochemical stations (in blue) and
803 the five reference cruise stations (in red).

804 **Figure 2.** Overview of the reference cruise spatial coverage and vertical distributions of the inorganic
805 nutrients. Top left: geographical distribution map, top right: vertical profiles of nitrate in $\mu\text{mol kg}^{-1}$,
806 bottom left: vertical profiles of phosphate in $\mu\text{mol kg}^{-1}$, bottom right: vertical profiles of silicate in
807 $\mu\text{mol kg}^{-1}$.

808 **Figure 3.** Scatter plots of (A.) phosphate vs nitrate (in $\mu\text{mol kg}^{-1}$) and (B.) silicate vs. nitrate (in μmol
809 kg^{-1}). Data that have been flagged as “questionable” (flag=3) are in red, the colour bar indicates the
810 pressure (in dbar). The black lines represent the best linear fit between the two parameters, and the
811 corresponding equations and r^2 values are shown on each plot. Average resulting N:P ratio is 20.87,
812 average resulting N:Si ratio is 1.05 (whole depth).

813 **Figure 4.** An example of the calculated offset for silicate between cruise 48UR20131015 and cruise
814 29AJ2016818 (reference cruise). Above: location of the stations being part of the crossover and
815 statistics. Bottom left: vertical profiles of silicate data in ($\mu\text{mol kg}^{-1}$) of the two cruises that fall within
816 the minimum distance criteria (the crossing region), below 1000 dbar. Bottom right: vertical plot of
817 the difference between both cruises (dotted black line) with standard deviations (dashed black lines)
818 and the weighted average of the offset (solid red line) with the weighted standard deviations (dotted
819 red line).

820 **Figure 5.** Results of the crossover analysis for nitrate, before (grey) and after adjustment (blue). Error
821 bars indicate the standard deviation of the absolute weighted offset. The dashed lines indicate the
822 accuracy limit 2% for an adjustment to be recommended.

823 **Figure 6.** The same as Fig. 5 but for phosphate.

824 **Figure 7.** The same as Fig. 5 but for silicate.

825 **Figure 8.** Dataset comparison before (black) and after (blue) adjustment, showing vertical profiles of
826 (A.) nitrate (in $\mu\text{mol kg}^{-1}$), (B.) phosphate (in $\mu\text{mol kg}^{-1}$) and (C.) silicate (in $\mu\text{mol kg}^{-1}$). Scatter plots
827 of the adjusted data from all depths after 1st and 2nd quality control for (D.) phosphate vs nitrate (in
828 $\mu\text{mol kg}^{-1}$) and (E.) silicate vs. nitrate (in $\mu\text{mol kg}^{-1}$). The black lines represent the best linear fit
829 between the two parameters, and the corresponding equations and r^2 values are shown on each plot.
830 Average resulting N:P ratio is 22.09, average resulting N:Si ratio is 0.94 (whole depth).

831 **Figure 9.** Vertical profiles of the inorganic nutrients in the dataset after adjustments and spatial
832 coverage of each cruise (reference to cruise ID is above each map). The whole WMED adjusted
833 product is shown in black while the data of each individual cruise are shown in blue (flag=2) and
834 green (flag=3).

835 **Figure 10.** RMSE regional averages of water mass properties computed between the new adjusted
836 product and MEDAR/Medatlas climatology for nitrate (A.), phosphate (B.) and silicate (C.).

837 **Table captions**

838 **Table 1a.** Cruise summary table and parameters listed with number of stations and samples. Cruises
839 were identified with an ID number and expedition code ('EXPOCODE' of format
840 AABBYYYMMDD with AA: country code, BB: ship code, YYYY: year, MM: month, DD: day
841 indicative of cruise starting day).

842 **Table 1b.** Data sources and links to the reports (accessed June 2020).

843 **Table 2.** Cruise summary table of the reference cruises collection used in the secondary quality
844 control, collected from 2001 to 2016.

845 **Table 3.** WOCE flags used in the original data product and in the adjusted product.

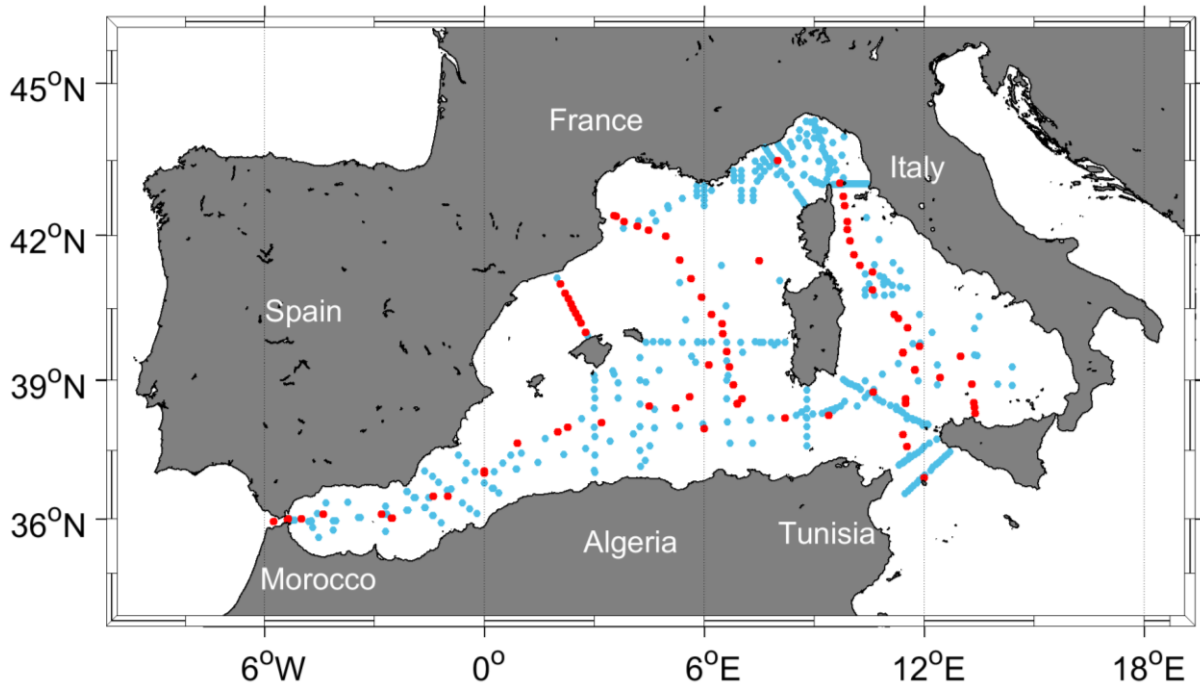
846 **Table 4.** Average and Standard deviations of nitrate, phosphate and silicate measurements by cruise
847 and for each region with number of samples deeper than 1000db included in the 2nd QC. Average
848 storage time: the minimum storage time defined as time difference between the cruise ending day and
849 the 1st day of the laboratory analysis.

850 **Table 5.** Summary of the suggested adjustment for nitrate, phosphate and silicate resulting from the
851 crossover analysis. Adjustments for inorganic nutrient are multiplicative. NA: denotes not adjusted,
852 i.e. data of cruises that could not be used in the crossover analysis, because of the lack of stations or
853 data are outside the spatial coverage of reference cruises.

854 **Table 6.** Secondary QC toolbox results: improvements of the weighted mean of absolute offset per
855 cruise of unadjusted and adjusted data; (n) is the number of crossovers per cruise. The numbers in red
856 (less than 1) indicate that the cruise data are lower than the reference cruises. NA: not adjusted.

857 **Table 7.** Water mass properties and regional average concentrations of inorganic nutrients:
858 comparison between the new adjusted product and the MEDAR/Medatlas climatology (with standard
859 deviations and number of observations in brackets).

860 **Figure 1**



861

862

863

864

865

866

867

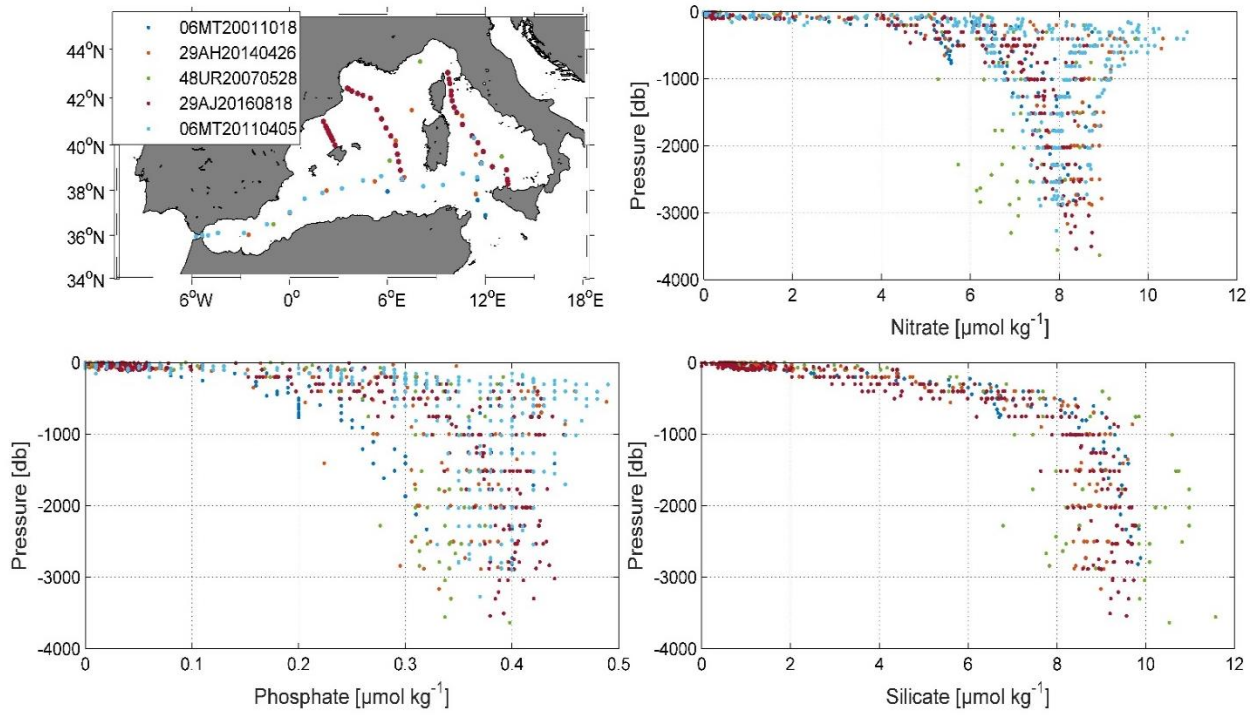
868

869

870

871

872 **Figure 2**



873

874

875

876

877

878

879

880

881

882

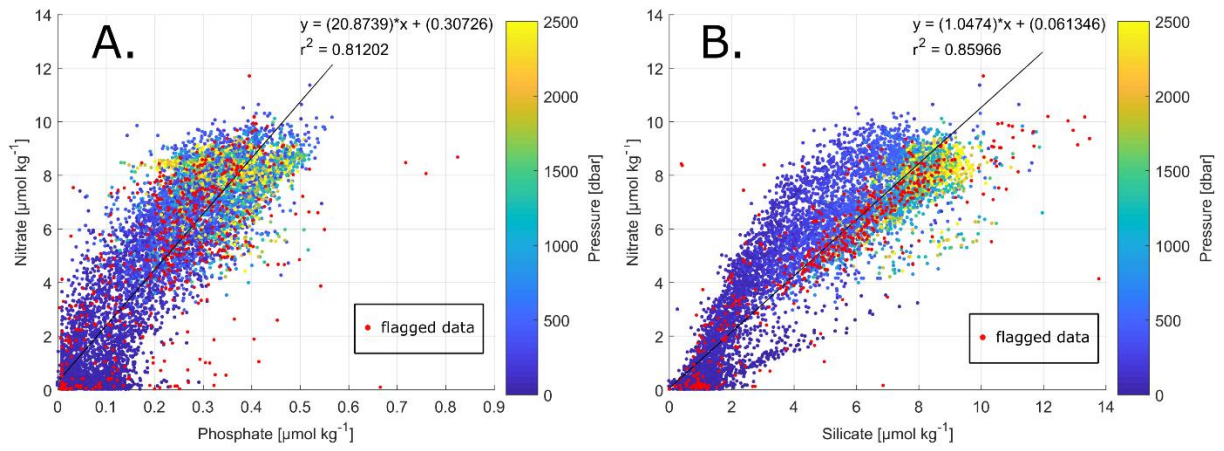
883

884

885

886

887 **Figure 3**



888

889

890

891

892

893

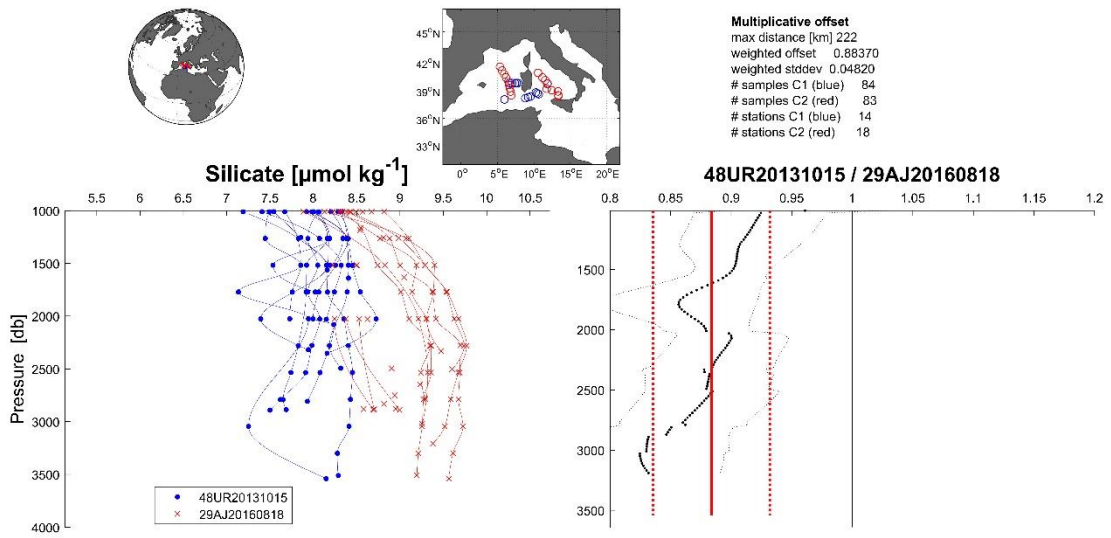
894 **Figure 4**

895

896

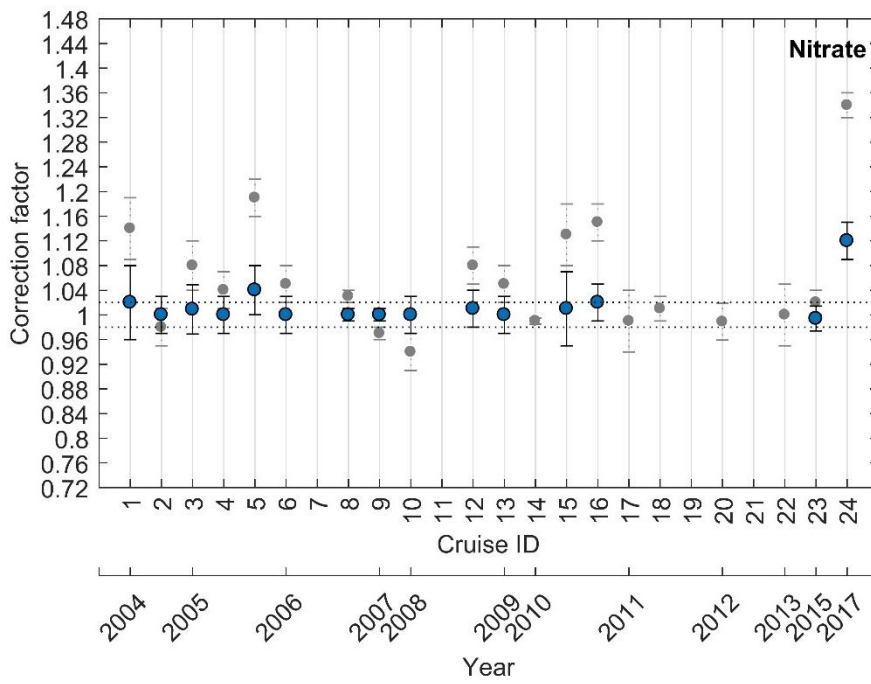
897

898



899

900 **Figure 5**



901

902

903

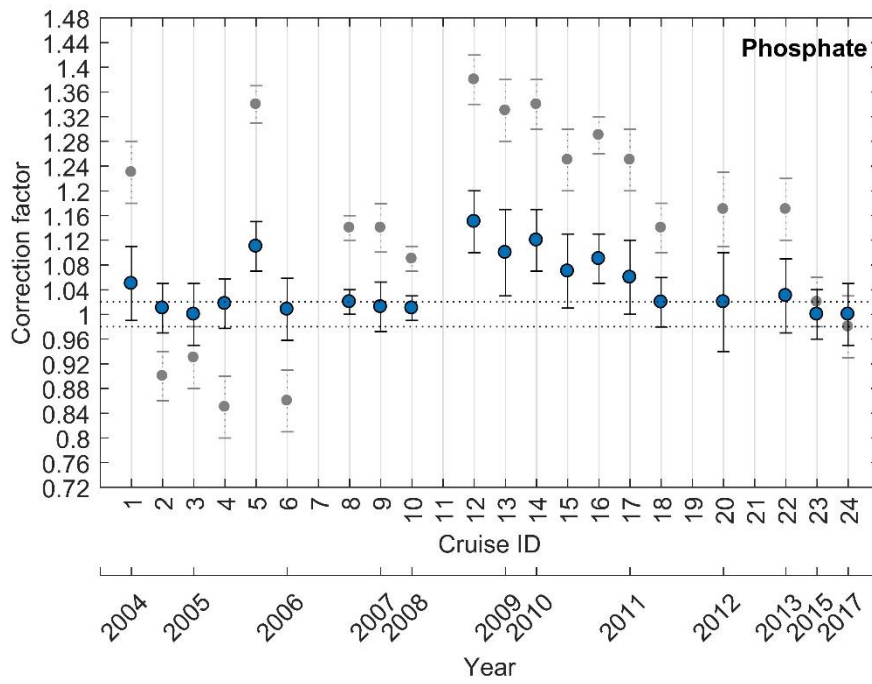
904

905

906

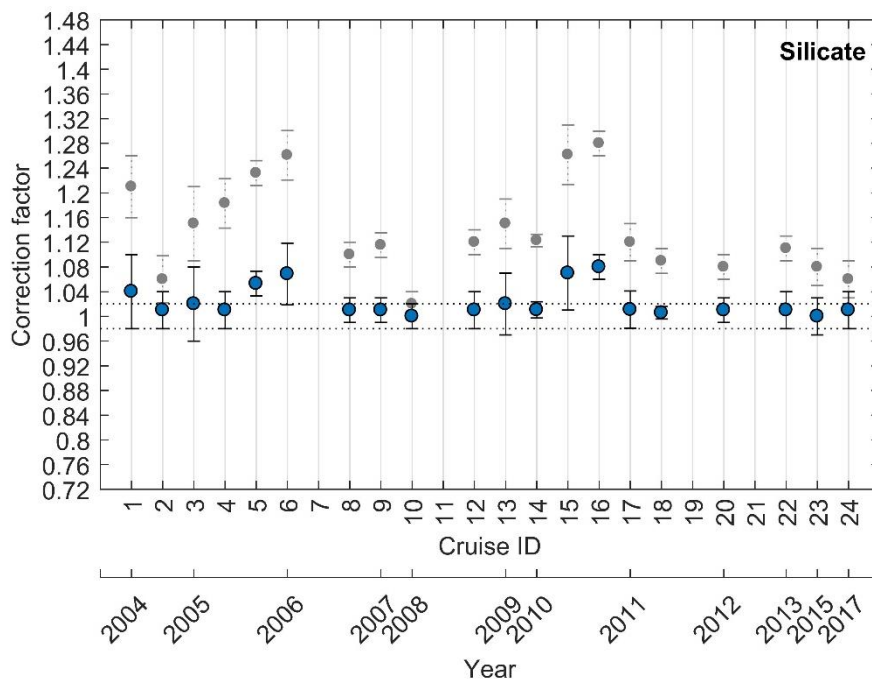
907
908
909
910
911
912
913
914
915
916

Figure 6



917
918
919
920
921
922

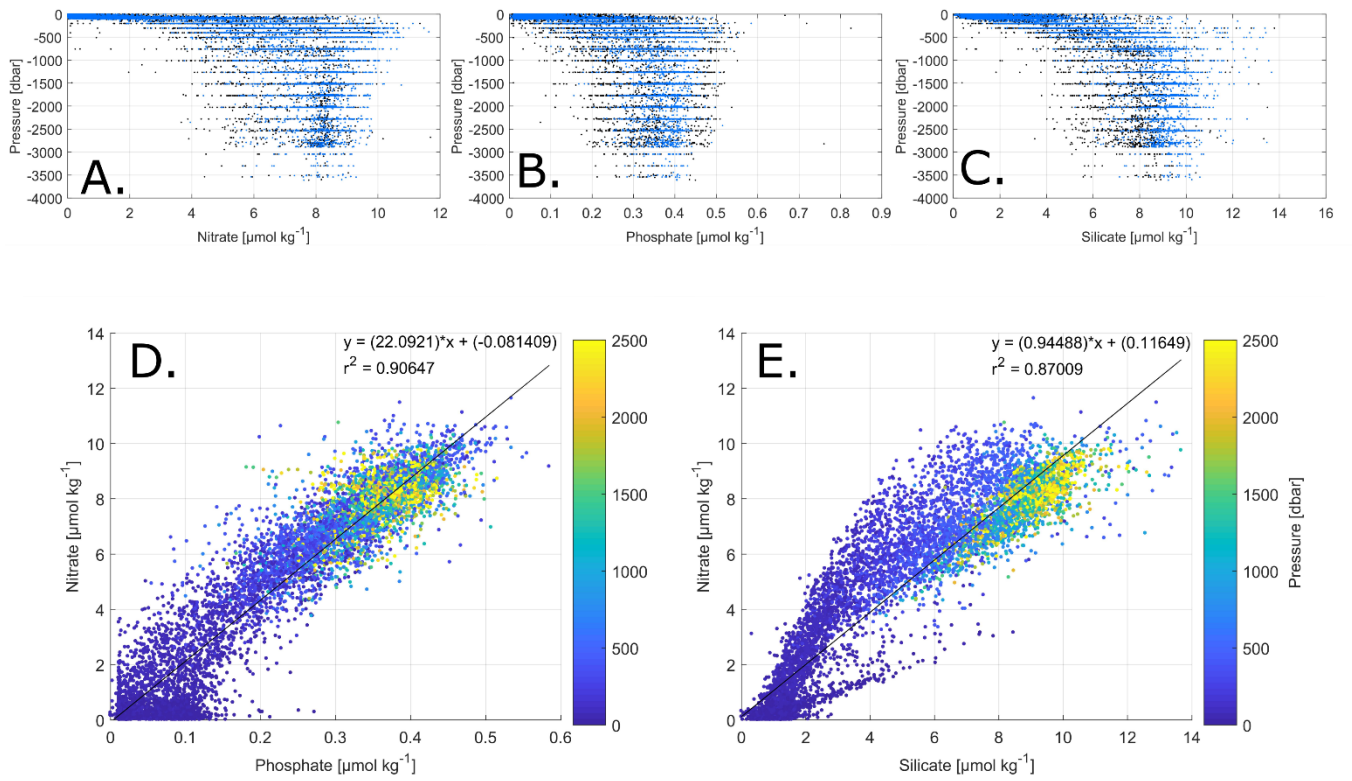
923
924
925
926
927
928
929
930
931
932 **Figure 7**



933
934
935
936
937
938

939
940
941
942
943
944
945
946
947
948

Figure 8



949
950
951
952
953

954

955

956

957

958

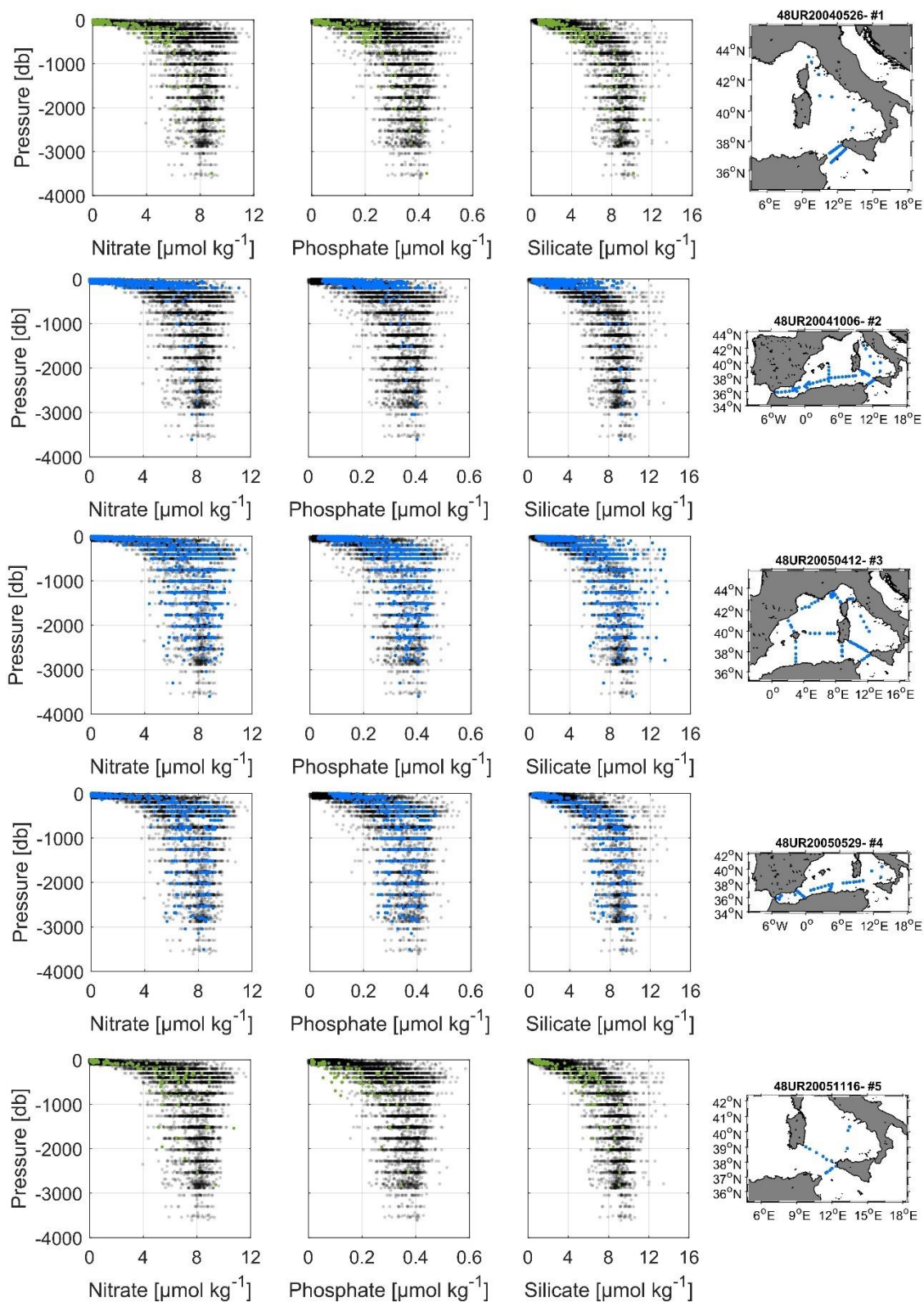
959

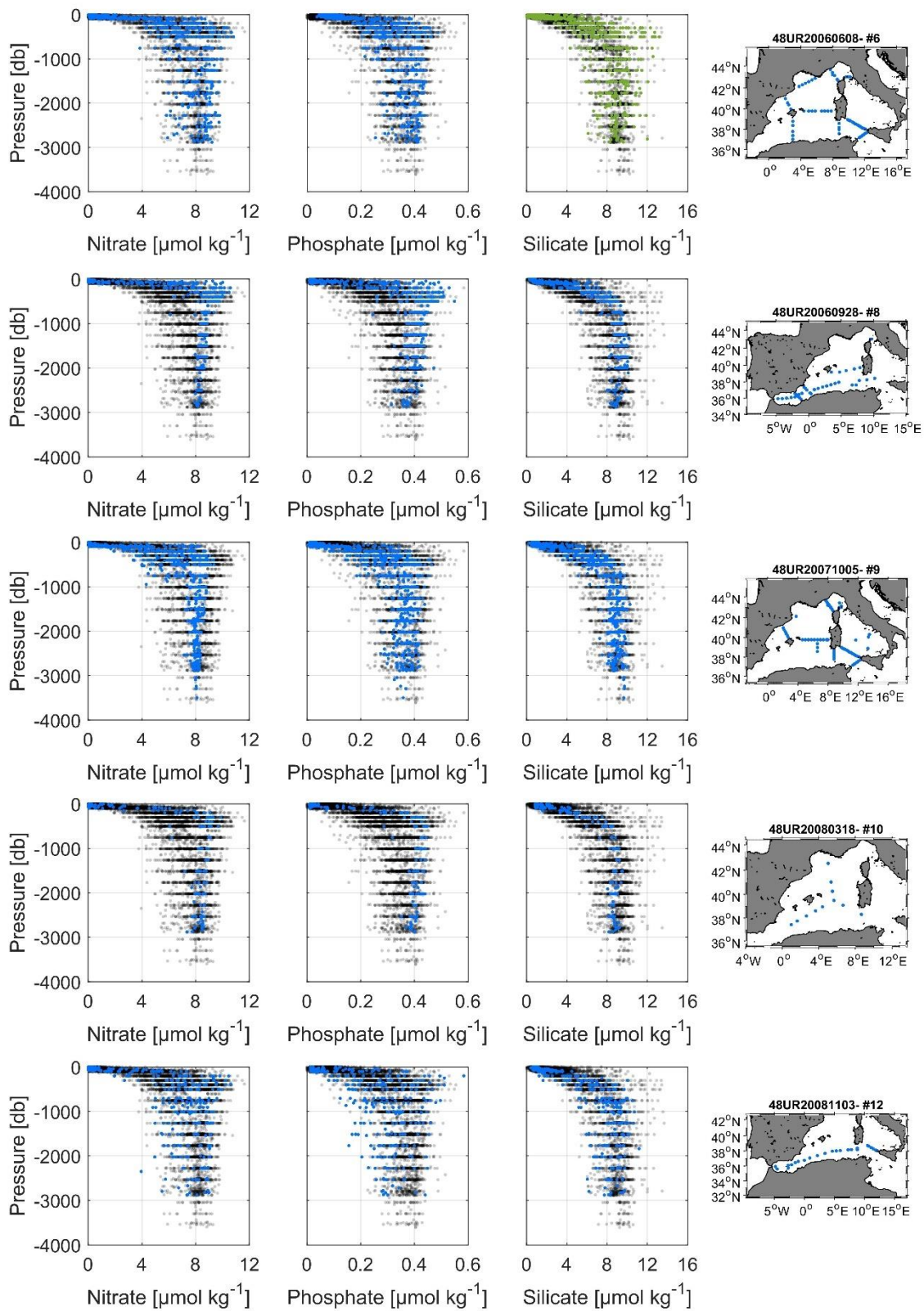
960

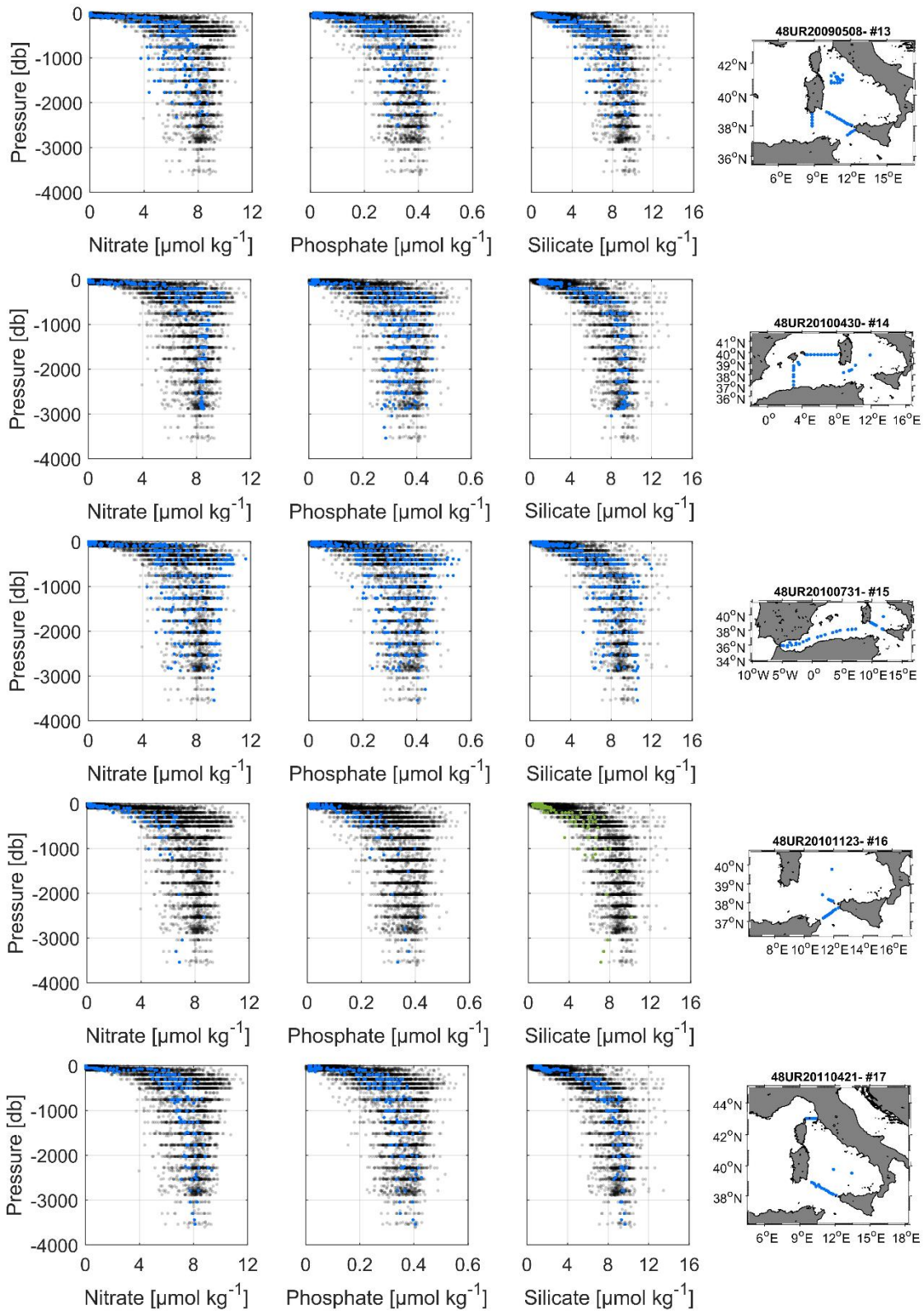
961

962

963 **Figure 9**

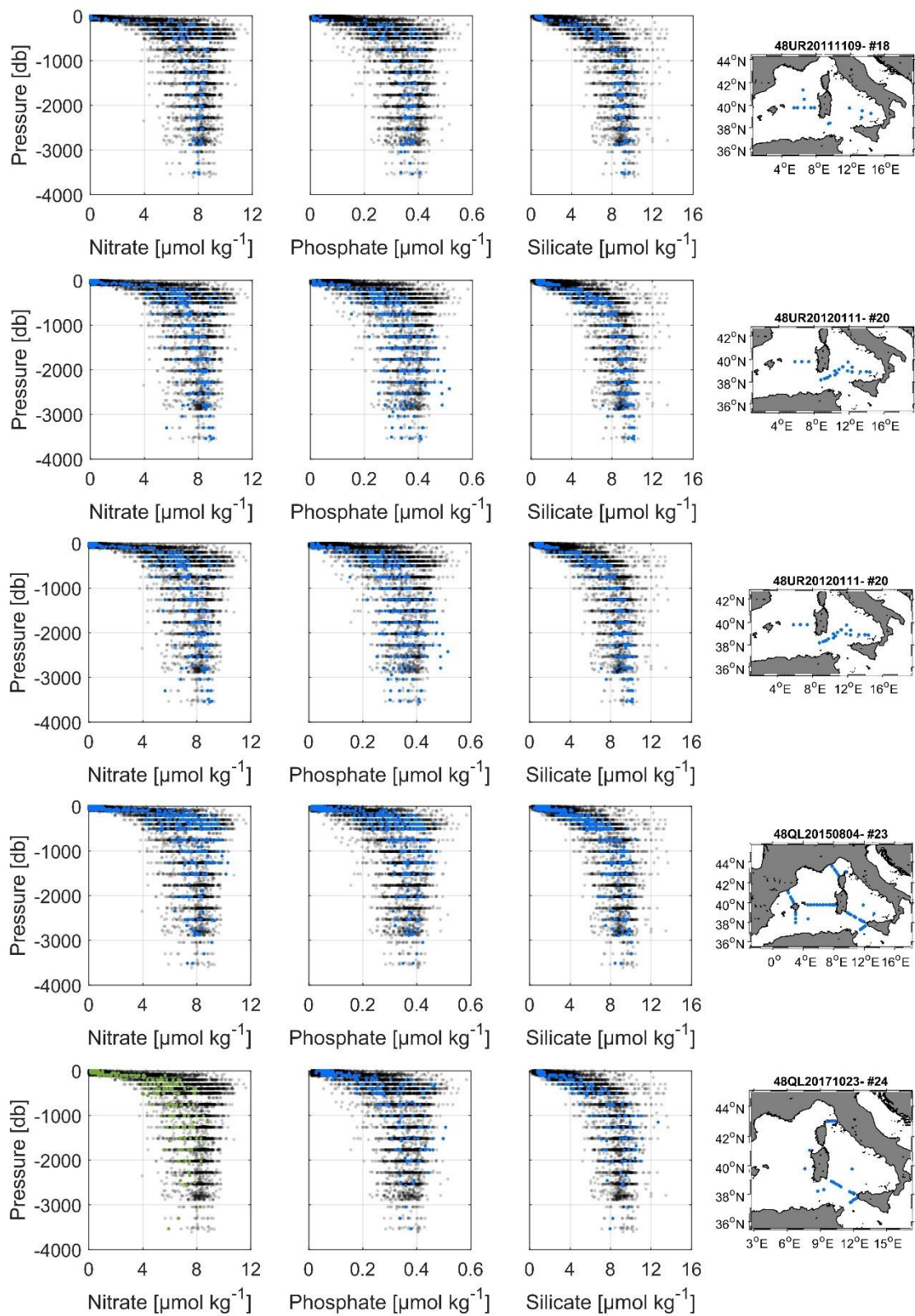






966

967

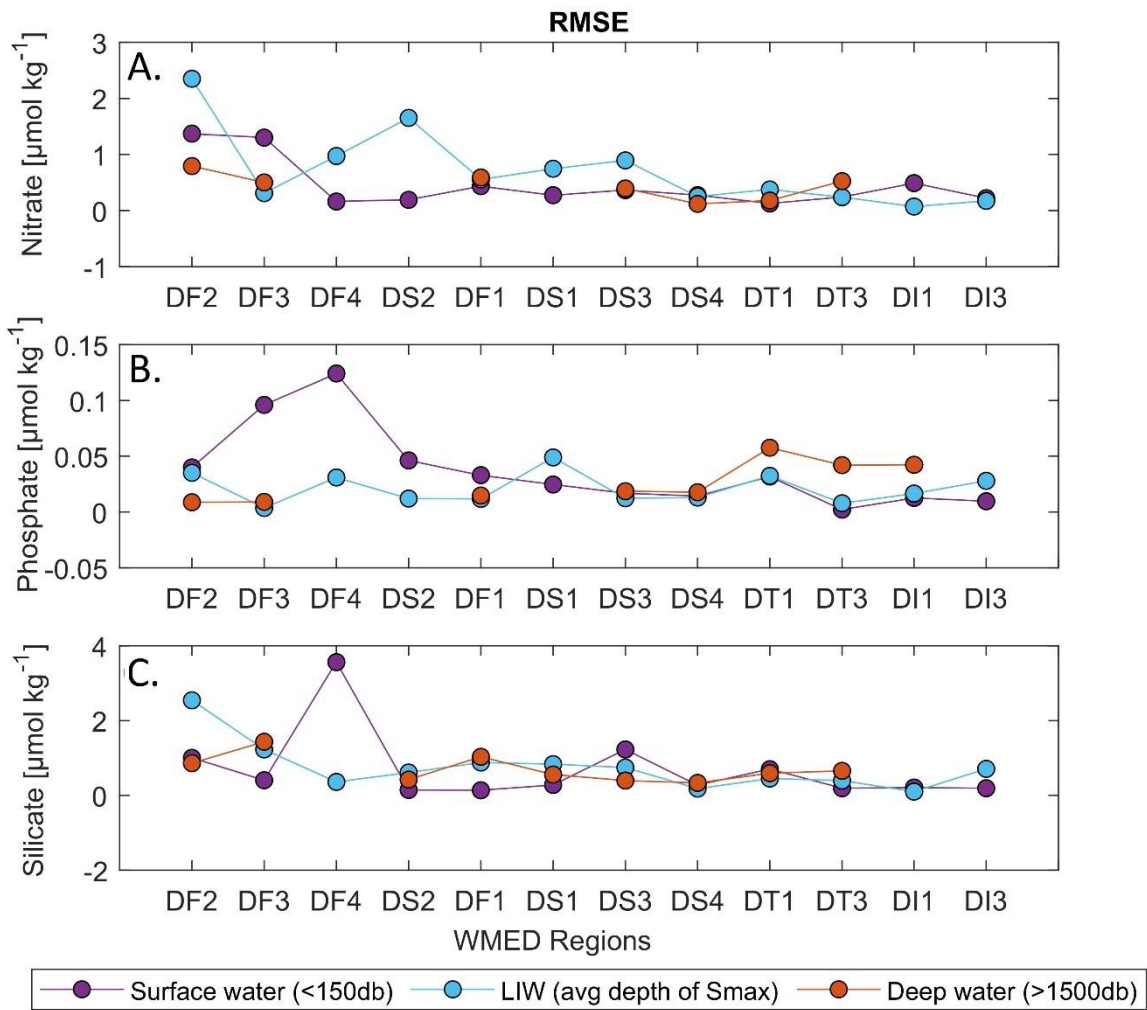


968

969

970 **Figure 10**

971



972

973

974

975

976

977

978

979

980

Table 1a

Cruise ID (#)	Common Name	EXPOCODE	Research vessel (RV)	Date Start/End	Stations	Samples Nitrate	Samples Phosphate	Samples Silicate	Maximum bottom depth (m)	Chief scientist
1	TRENDS2004/MEDGOOS8leg2	48UR20040526	Urania	26 MAY - 14 JUN 2004	36	255	253	255	3499	M. Borghini
2	MEDGOOS9	48UR20041006	Urania	6 - 25 OCT 2004	68	627	626	627	3610	M. Borghini
3	MEDOCC05/MFSTEP2	48UR20050412	Urania	12 APR - 16 MAY 2005	68	828	828	828	3598	M. Borghini
4	MEDGOOS10	48UR20050529	Urania	29 MAY - 10 JUN 2005	36	577	577	577	3505	A. Perilli
5	MEDGOOS11	48UR20051116	Urania	16 NOV - 3 DEC 2005	14	143	143	143	2810	A. Perilli, M. Borghini, M. Dibitto
6	MEDOCC06	48UR20060608	Urania	8 JUN - 3 JUL 2006	66	787	785	787	2881	M. Borghini
7	SIRENA06	06A420060720	NRV Alliance	20 JUL - 6 AUG 2006	35	208	208	209	1854	J. Haun
8	MEDGOOS13/MEDBIO06	48UR20060928	Urania	28 SEP - 8 NOV 2006	37	519	520	520	2862	A. Ribotti
9	MEDOCC07	48UR20071005	Urania	5 - 29 OCT 2007	71	977	977	979	3497	A. Perilli, M. Borghini
10	SESAMEIt4	48UR20080318	Urania	18 MAR - 7 APR 2008	11	164	164	164	2882	A. Ribotti
11	SESAMEIt5	48UR20080905	Urania	5 - 16 SEP 2008	12	74	74	74	536	C. Santinelli
12	MEDCO08	48UR20081103	Urania	3 - 24 NOV 2008	24	342	350	348	2880	S. Sparnocchia, G.P. Gasparini, M. Borghini
13	TYRRMOUNTS	48UR20090508	Urania	8 MAY - 3 JUN 2009	41	430	441	440	2559	A. Ribotti
14	BIOFUN010	48UR20100430	Urania	30 APR - 17 MAY 2010	26	405	405	405	3540	G.P. Gasparini
15	VENUS1	48UR20100731	Urania	31 JUL - 25 AUG 2010	32	431	432	428	3544	E. Manini, S. Aliani
16	BONSIC2010	48UR20101123	Urania	23 NOV - 9 DEC 2010	18	144	143	143	3540	G.P. Gasparini, M. Borghini
17	EUROFLEET11	48UR20110421	Urania	21 APR - 8 MAY 2011	28	277	275	277	3540	A. Ribotti
18	BONIFACIO2011	48UR20111109	Urania	9 - 23 NOV 2011	13	180	180	181	3541	G.P. Gasparini, M. Borghini
19	TOSCA2011	48MG20111210	Maria Grazia	10 - 20 DEC 2011	21	310	310	309	2728	A. Ribotti, G. La Spada, M. Borghini
20	ICHNUSSA12	48UR20120111	Urania	11 - 27 JAN 2012	21	353	352	323	3551	M. Borghini
21	EUROFLEET2012	48UR20121108	Urania	8 - 26 NOV 2012	53	429	434	434	2633	A. Ribotti
22	ICHNUSSA13	48UR20131015	Urania	15 - 29 OCT 2013	37	405	404	405	3540	J. Chiggiato
23	OCEANCERTAIN15	48QL20150804	Minerva Uno	4 - 29 AUG 2015	71	531	531	531	3513	A. Ribotti, S. Sparnocchia, M. Borghini
24	ICHNUSSA17/INFRAOCE17	48QL20171023	Minerva Uno	23 OCT - 28 NOV 2017	31	251	254	254	3536	

Table 1b

Cruise ID (#)	Expedition original Name	PIs/ Chief scientist	Specific link* (accessed June 2020)
1	TRENDS2004/ MEDGOOS8leg2	M. Borghini	https://isramar.ocean.org.il/perseus_data/CruiseInfo.aspx?criuseid=5821 https://isramar.ocean.org.il/perseus_data/CruiseInfo.aspx?criuseid=4935
2	MEDGOOS9	M. Borghini	Report submission in progress https://isramar.ocean.org.il/perseus_data/CruiseInfo.aspx?criuseid=5823 https://doi.org/10.17882/70340
3	MEDOCC05/ MFSTEP2	M. Borghini	http://ricerca.ismar.cnr.it/CRUISE_REPORTS/2005/URANIA_MEDOCC05.pdf https://isramar.ocean.org.il/perseus_data/CruiseInfo.aspx?criuseid=4936
4	MEDGOOS10	A. Perilli	http://www.seaforecast.cnr.it/it/observation_it.htm https://doi.org/10.17882/70340
5	MEDGOOS11	A. Perilli, M. Borghini, M. Dibitetto	http://ricerca.ismar.cnr.it/CRUISE_REPORTS/2005/URANIA_MEDGOOS11_05_REP.pdf https://doi.org/10.17882/70340
6	MEDOCC06	M. Borghini	http://www.seaforecast.cnr.it/reports/Medocc06CR.pdf https://seadata.bsh.de/Cgi-csr/retrieve_sdn2/viewReport.pl?csrref=20106010
7	SIRENA06	J. Haun	Report submission in progress
8	MEDGOOS13/ MEDBIO06	A. Ribotti	http://www.seaforecast.cnr.it/reports/Mebio06-Medg13_CR.pdf https://doi.org/10.17882/70340
9	MEDOCC07	A. Perilli, M. Borghini, A. Ribotti	http://www.seaforecast.cnr.it/reports/Medocc07-MedCo07_Rapp.pdf https://isramar.ocean.org.il/perseus_data/CruiseInfo.aspx?criuseid=5146
10	SESAMEIt4	C. Santinelli	https://isramar.ocean.org.il/perseus_data/CruiseInfo.aspx?criuseid=5148 https://emodnet-chemistry.maris.nl/search/details.php?step=0012004~0022017~0153~057104001~058tdin_ntra_phos_slca~00445~0056~00617~00734~0541&count=3592&page=1000&sort=0&header=no https://isramar.ocean.org.il/perseus_data/CruiseInfo.aspx?criuseid=5147
11	SESAMEIT5	S. Sparnocchia, G.P. Gasparini, M. Borghini	https://isramar.ocean.org.il/perseus_data/CruiseInfo.aspx?criuseid=5147
12	MEDCO08	A. Ribotti	http://www.seaforecast.cnr.it/reports/MedCO08_Rapp.pdf
13	TYRRMOUNTS	G.P. Gasparini	Report submission in progress
14	BIOFUN010	E. Manini, S. Aliani	http://www.ismar.cnr.it/products/reports-campagne/2010-2019
15	VENUS1	G.P. Gasparini, M. Borghini	Report submission in progress
16	BONSIC2010	A. Ribotti	http://www.seaforecast.cnr.it/reports/Bonifacio2010Sic_Rapp.pdf
17	EUROFLEET11	G.P. Gasparini, M. Borghini	Report submission in progress
18	BONIFACIO2011	A. Ribotti, G. La Spada, M. Borghini	http://www.seaforecast.cnr.it/reports/Bonifacio2011_Rapp.pdf
19	TOSCA2011	M. Borghini	Report submission in progress
20	ICHNUSSA12	A. Ribotti	http://www.seaforecast.cnr.it/reports/Ichnussa2012_Rapp.pdf
21	EUROFLEET2012	M. Borghini	Report submission in progress
22	ICHNUSSA13	A. Ribotti	http://www.seaforecast.cnr.it/reports/Ichnussa2013_Rapp.pdf
23	OCEANCERTAIN15	J. Chiggiato	https://doi.pangaea.de/10.1594/PANGAEA.911046
24	ICHNUSSA17/ INFRAOCE17	A. Ribotti, S. Sparnocchia, M. Borghini	Report submission in progress

* The specific links are subjected to updates.

Table 2

Common name	EXPOCODE	Date Start/End	Stations	Nitrate Sample	Phosphate Sample	Silicate Sample	Source	Nutrient PI	Chief scientist
<i>M51/2</i>	06MT20011018	18 OCT - 11 NOV 2001	6	79	79	82	GLODAPv2	B. Schneider	W. Roether
<i>TRANSMED_LEGII</i>	48UR20070528	28 MAY - 12 JUN 2007	4	78	77	78	CARIMED (not yet available)	S. Cozzi, V. Ibello	M. Azzaro
<i>M84/3</i>	06MT20110405	5 - 28 APR 2011	20	339	343	-	GLODAPv2	G. Civitarese	T. Tanhua
<i>HOTMIX</i>	29AH20140426	26 APR - 31 MAY 2014	18	144	140	144	CARIMED (not yet available)	XA Álvarez-Salgado	J. Aristegui
<i>TALPro-2016</i>	29AJ20160818	18 - 28 AUG 2016	42	293	293	293	MedSHIP programme	L. Coppola	L. Jullion, K. Schroeder

Table 3

WOCE flag value	Interpretation in original dataset	Interpretation in adjusted product
2	Acceptable/ measured	Adjusted and acceptable
3	Questionable/not used	Adjusted and recommended questionable
9	not measured/no data	-

Table 4

Cruise ID	EXPOCODE/ Region	Regional Avg Nitrate (μmol)	std Nitrate	Regional Avg Phosphate	std Phosphate(Regional Avg Silicate (μmol)	std Silicate	# samples	Avg storage (in
-----------	------------------	--	-------------	------------------------	----------------	---	--------------	-----------	-----------------

		kg ⁻¹)	(μmol kg ⁻¹)	(μmol kg ⁻¹)	μmol kg ⁻¹)	kg ⁻¹)	(μmol kg ⁻¹)	days)	
1	48UR20040526/ <i>DT1-Tyrrhenian North</i> <i>DT3-Tyrrhenian South</i>	6.07 7.03	1.25 1.32 0.51	0.26 0.31	0.062 0.065 0.02	6.92 7.66	1.64 1.83 0.53	21 16 5	131
2	48UR20041006/ <i>DT1-Tyrrhenian North</i> <i>DT3-Tyrrhenian South</i>	7.68 8.17	0.59 0.53 0.60	0.41 0.41	0.029 0.031 0.025	8.74 9.31	0.81 0.75 0.87	21 15 6	251
3	48UR20050412/ <i>DF2-Gulf of Lion</i> <i>DF3-Liguro-Provençal</i> <i>DS2-Balearic Sea</i> <i>DF1-Algero-Provençal</i> <i>DS3-Algerian West</i> <i>DT1-Tyrrhenian North</i> <i>DT3-Tyrrhenian South</i> <i>DII-Sardinia Channel</i>	7.89 7.45 7.44 7.87 7.7 6.57 6.52 7.22	1.15 0.98 1.08 1.14 1.16 1.065 1.12 1.065	0.40 0.41 0.40 0.41 0.39 0.36 0.36 0.40	0.050 0.044 0.05 0.043 0.048 0.047 0.05 0.04	8.17 7.72 7.68 8.88 8.14 7.41 7.56 8.08	1.41 1.065 1.10 1.47 1.96 1.15 1.42 1.11	233 24 66 42 23 21 22 14	135
4	48UR20050529/ <i>DS1-Alboran Sea</i> <i>DS3-Algerian West</i> <i>DS4-Algerian East</i> <i>DT1-Tyrrhenian North</i> <i>DT3-Tyrrhenian South</i> <i>DII-Sardinia Channel</i>	6.4 7.6 7.48 7.24 7.70 7.58	1.13 1.15 1.13 1.13 0.44 1.08	0.38 0.41 0.41 0.42 0.41 0.43	0.057 0.041 0.06 0.06 0.03 0.049	6.26 7.33 7.50 7.91 7.55 7.42	1.08 1.02 0.99 1.23 0.56 0.82	205 32 73 16 14 23	314
5	48UR20051116/ <i>DT1-Tyrrhenian North</i> <i>DT3-Tyrrhenian South</i> <i>DII-Sardinia Channel</i>	5.68 6.71 6.29	1.35 1.26 1.51 0	0.19 0.20 0.26	0.078 0.08 0.06 0	6.30 6.86 7.53	0.98 0.92 1.065 0	16 10 5 1	738
6	48UR20060608/ <i>DF2-Gulf of Lion</i> <i>DF3-Liguro-Provençal</i> <i>DS2-Balearic Sea</i> <i>DF1-Algero-Provençal</i> <i>DS3-Algerian West</i> <i>DT3-Tyrrhenian South</i> <i>DII-Sardinia Channel</i>	7.69 8.08 8.06 7.97 8.39 6.39 8.04	1.16 1.02 0.78 0.9 1.16 0.9 0.85	0.42 0.43 0.43 0.44 0.42 0.36 0.43	0.054 0.04 0.04 0.03 0.05 0.03 0.04	7.089 7.41 7.07 7.34 8.5 6.86 7.77	1.47 1.04 1.21 1.18 1.32 2 1.7 1.25	221 27 35 30 61 28 26 14	27
7	06A420060720	-	-	-	-	-	-	-	1367
8	48UR20060928/ <i>DS2-Balearic Sea</i> <i>DF1-Algero-Provençal</i> <i>DS1-Alboran Sea</i> <i>DS3-Algerian West</i> <i>DS4-Algerian East</i> <i>DT3-Tyrrhenian South</i> <i>DII-Sardinia Channel</i>	7.97 8.17 8.2 7.93 7.98 6.2 7.66	0.71 0.17 0.22 0.14 0.89 0.68 0.6	0.33 0.33 0.35 0.33 0.34 0.28 0.28	0.036 0.017 0.026 0.02 0.03 0.04 0.02	7.84 8.11 8.59 8.09 8.01 6.71 8.00	0.76 0.27 0.3 0.35 0.91 0.7 1.45 0.49	179 4 22 47 70 3 5	606
9	48UR20071005/ <i>DF2-Gulf of Lion</i> <i>DF3-Liguro-Provençal</i> <i>DS2-Balearic Sea</i> <i>DF1-Algero-Provençal</i> <i>DS4-Algerian East</i> <i>DT1-Tyrrhenian North</i> <i>DT3-Tyrrhenian South</i> <i>DII-Sardinia Channel</i>	8.41 8.17 8.17 8.33 8.41 7.83 7.49 7.92	0.89 0.08 1.08 0.43 0.6 0.2 1.05	0.31 0.31 0.31 0.32 0.33 0.28 0.28 0.33	0.040 0.01 0.03 0.02 0.018 0.03 0.05 0.02	7.43 7.64 7.58 7.79 7.90 8.26 7.71 8.26	0.86 0.02 1.08 0.39 0.69 0.26 1.26 0.41	302 4 81 29 82 19 26 38 23	751
10	48UR20080318/ <i>DF2-Gulf of Lion</i> <i>DS2-Balearic Sea</i> <i>DF1-Algero-Provençal</i> <i>DS3-Algerian West</i> <i>DS4-Algerian East</i> <i>DII-Sardinia Channel</i>	8.54 9.12 9.02 8.93 8.43 7.62	0.51 0.6 0.18 0.36 0.46 0.25 0.6	0.35 0.38 0.38 0.36 0.38 0.34	0.026 0.03 0.01 0.03 0.01 0.02 0.03	8.62 8.40 8.65 8.69 8.32 8.49	0.34 0.43 0.21 0.25 0.35 0.22 0.36	66 5 9 15 20 10 3	31
11*	48UR20080905	-	-	-	-	-	-	-	211
12	48UR20081103/ <i>DS1-Alboran Sea</i> <i>DS3-Algerian West</i> <i>DS4-Algerian East</i> <i>DT3-Tyrrhenian South</i> <i>DII-Sardinia Channel</i>	6.4 7.58 7.15 7.44 7.40	1.11 1.21 0.9 1.04 1.23	0.21 0.27 0.23 0.22 0.17	0.077 0.06 0.1 0.04 0.05 0.04	7.20 7.89 7.38 8.28 8.09	0.10 1.43 0.9 0.9 0.45	110 26 30 10 9	536
13	48UR20090508/ <i>DT1-Tyrrhenian North</i> <i>DT3-Tyrrhenian South</i> <i>DII-Sardinia Channel</i>	5.95 6.76 7.62	1.41 1.55 0.77 1.1	0.24 0.24 0.28	0.051 0.05 0.03 0.05	6.28 7.37 7.76	1.42 1.58 0.77 0.9	88 46 29 13	164
14	48UR20100430/ <i>DS2-Balearic Sea</i> <i>DF1-Algero-Provençal</i>	7.66 8.43	1.06 1.6 0.29	0.25 0.26	0.036 0.03 0.03	7.38 8.06	1.03 1.75 0.31	159 33 61	213

	<i>DS3-Algerian West</i>	8.5	0.14	0.26	0.03	8.25	0.3	26	
	<i>DT1-Tyrrhenian North</i>	6.88	0.8	0.23	0.022	7.17	0.77	11	
	<i>DT3-Tyrrhenian South</i>	6.38	1.35	0.22	0.01	6.76	1.56	7	
	<i>DII-Sardinia Channel</i>	7.71	0.87	0.23	0.02	7.80	0.74	21	
15	48UR20100731/		1.34		0.053		0.14	149	213
	<i>DS1-Alboran Sea</i>	7.30	1.18	0.29	0.05	7.21	1.11	25	
	<i>DS3-Algerian West</i>	7.67	1.15	0.28	0.045	7.24	1.16	54	
	<i>DS4-Algerian East</i>	7.38	0.89	0.29	0.03	7.00	0.78	29	
	<i>DT1-Tyrrhenian North</i>	7.66	0.96	0.29	0.05	7.89	1.07	10	
	<i>DT3-Tyrrhenian South</i>	5.4	0.67	0.22	0.01	5.52	1.56	30	
	<i>DII-Sardinia Channel</i>	4.92	0	0.20	0	5.55	0	1	
16	48UR20101123/		1.02		0.045		1.02	14	170
	<i>DT1-Tyrrhenian North</i>	6.34	0.87	0.27	0.02	6.12	0.87	8	
	<i>DT3-Tyrrhenian South</i>	5.43	1.02	0.22	0.04	5.08	0.9	6	
17	48UR20110421/		0.62		0.029		0.52	56	160
	<i>DT1-Tyrrhenian North</i>	7.77	0.45	0.28	0.02	8.11	0.35	21	
	<i>DT3-Tyrrhenian South</i>	7.76	0.7	0.28	0.03	8.017	0.6	35	
18	48UR20111109/		0.68		0.025		0.70	77	74
	<i>DF3-Liguro-Provençal</i>	6.68	0	0.33	0	6.26	0	1	
	<i>DF1-Algero-Provençal</i>	8.17	0.5	0.32	0.01	8.16	0.66	43	
	<i>DT1-Tyrrhenian North</i>	7.26	0.93	0.29	0.02	8.15	1.03	12	
	<i>DT3-Tyrrhenian South</i>	7.61	0.37	0.30	0.02	8.18	0.35	11	
	<i>DII-Sardinia Channel</i>	7.64	0.45	0.29	0.01	8.08	0.41	10	
19*	48MG20111210		-		-		-	-	38
20	48UR20120111/		0.97		0.051		0.26	152	317
	<i>DF1-Algero-Provençal</i>	8.45	0.49	0.31	0.039	7.91	0.53	23	
	<i>DT1-Tyrrhenian North</i>	7.67	0.83	0.27	0.02	8.29	0.8	30	
	<i>DT3-Tyrrhenian South</i>	7.65	1.06	0.31	0.06	8.03	1.26	69	
	<i>DII-Sardinia Channel</i>	7.65	0.96	0.31	0.03	7.86	0.78	30	
21*	48UR20121108		-		-		-	-	72
22	48UR20131015/		1.03		0.043		0.79	98	76
	<i>DF1-Algero-Provençal</i>	8.54	0.64	0.33	0.02	7.96	0.38	36	
	<i>DS4-Algerian East</i>	7.67	1.28	0.27	0.04	6.82	1.07	8	
	<i>DT1-Tyrrhenian North</i>	6.47	0.83	0.24	0.025	7.12	0.84	10	
	<i>DT3-Tyrrhenian South</i>	7.81	0.71	0.30	0.03	8.09	0.65	28	
	<i>DII-Sardinia Channel</i>	7.32	0.99	0.27	0.02	7.47	0.89	16	
23	48QL20150804/		0.84		0.038		0.85	94	30
	<i>DF3-Liguro-Provençal</i>	8.51	0.96	0.39	0.03	8.06	0.85	23	
	<i>DS2-Balearic Sea</i>	7.75	0.66	0.36	0.02	7.86	0.81	20	
	<i>DF1-Algero-Provençal</i>	7.9	0.59	0.37	0.03	8.34	0.68	23	
	<i>DS3-Algerian West</i>	7.84	0.67	0.36	0.02	7.75	0.68	6	
	<i>DT1-Tyrrhenian North</i>	7.92	0.61	0.37	0.02	8.75	0.4	8	
	<i>DT3-Tyrrhenian South</i>	7.23	0.75	0.34	0.025	8.2	0.94	13	
	<i>DII-Sardinia Channel</i>	6.30	0	0.25	0	5.36	0	1	
24	48QL20171023/		0.68		0.055		1.24	55	30
	<i>DF3-Liguro-Provençal</i>	6.63	0.41	0.40	0.05	10.76	1.07	3	
	<i>DF1-Algero-Provençal</i>	5.14	0.7	0.43	0.02	7.94	1.19	6	
	<i>DT1-Tyrrhenian North</i>	4.98	0.58	0.36	0.02	8.10	0.87	9	
	<i>DT3-Tyrrhenian South</i>	5.43	0.5	0.36	0.04	9.03	0.87	26	
	<i>DII-Sardinia Channel</i>	5.16	0.76	0.41	0.07	7.58	1.17	11	

(*) cruise not included in the 2ndQC (Section 4.)

in bold: the overall standard deviation by cruise; in normal font: regional standard deviation by cruise

Table 5

Cruise ID	EXPOCODE	Nitrate (x)	Phosphate (x)	Silicate (x)
1	48UR20040526	1.14	1.23	1.21
2	48UR20041006	0.98	0.9	1.06
3	48UR20050412	1.08	0.93	1.15
4	48UR20050529	1.04	0.85	1.183
5	48UR20051116	1.19	1.34	1.232

6	48UR20060608	1.05	0.86	1.261
7	06A420060720*	-	-	-
8	48UR20060928	1.03	1.14	1.1
9	48UR20071005	0.97	1.14	1.115
10	48UR20080318	0.94	1.09	1.02
11	48UR20080905*	-	-	-
12	48UR20081103	1.08	1.38	1.12
13	48UR20090508	1.05	1.33	1.15
14	48UR20100430	NA	1.34	1.123
15	48UR20100731	1.13	1.25	1.262
16	48UR20101123	1.15	1.29	1.28
17	48UR20110421	NA	1.25	1.12
18	48UR20111109	NA	1.14	1.09
19	48MG20111210*	-	-	-
20	48UR20120111	NA	1.17	1.08
21	48UR20121108*	-	-	-
22	48UR20131015	NA	1.17	1.11
23	48QL20150804	1.02	1.02	1.08
24	48QL20171023	1.34	0.98	1.06

(*) cruise not included in the 2ndQC (Section 4.)

Table 6

Cruise ID	EXPOCODE	Nitrate [%]			Phosphate[%]			Silicate[%]		
		<i>n</i>	<i>unadjusted</i>	<i>adjusted</i>	<i>n</i>	<i>unadjusted</i>	<i>adjusted</i>	<i>n</i>	<i>unadjusted</i>	<i>adjusted</i>
1	48UR20040526	2	0.86	0.98	2	0.77	0.95	1	0.79	0.96
2	48UR20041006	2	1.02	1.00	2	1.10	0.99	1	0.94	0.99
3	48UR20050412	5	0.92	0.99	5	1.07	1.00	4	0.85	0.98
4	48UR20050529	5	0.96	1.00	5	1.15	0.98	4	0.82	0.99
5	48UR20051116	2	0.81	0.96	1	0.66	0.89	1	0.77	0.95
6	48UR20060608	5	0.95	1.00	5	1.14	0.99	4	0.74	0.93
7	06A420060720	0	-	-	0	-	-	0	-	-
8	48UR20060928	4	0.97	1.00	4	0.86	0.98	3	0.90	0.99
9	48UR20071005	5	1.03	1.00	5	0.86	0.98	4	0.88	0.99
10	48UR20080318	3	1.06	1.00	3	0.91	0.99	2	0.98	1.00
11	48UR20080905	0	-	-	0	-	-	0	-	-
12	48UR20081103	5	0.92	0.99	5	0.62	0.85	4	0.88	0.99
13	48UR20090508	3	0.95	1.00	3	0.67	0.90	2	0.85	0.98
14	48UR20100430	4	1.01	NA	4	0.66	0.88	3	0.88	0.99
15	48UR20100731	5	0.87	0.99	5	0.75	0.93	4	0.74	0.93
16	48UR20101123	1	0.85	0.98	1	0.71	0.91	1	0.72	0.92
17	48UR20110421	2	1.01	NA	2	0.75	0.94	1	0.88	0.99
18	48UR20111109	4	0.99	NA	4	0.86	0.98	3	0.91	0.99
19	48MG20111210	0	-	-	0	-	-	0	-	-
20	48UR20120111	4	1.01	NA	4	0.83	0.98	3	0.92	0.99
21	48UR20121108	0	-	-	0	-	-	0	-	-
22	48UR20131015	4	1.00	NA	4	0.83	0.97	3	0.89	0.99
23	48QL20150804	5	0.98	1.00	5	0.98	1.00	4	0.92	1.00
24	48QL20171023	3	0.66	0.88	3	1.02	1.00	2	0.94	0.99

red: data lower than reference

Table 7

Region/ Water mass	Nitrate ($\mu\text{mol kg}^{-1}$)		Phosphate ($\mu\text{mol kg}^{-1}$)		Silicate ($\mu\text{mol kg}^{-1}$)	
	Avg new Product	Avg Medar	Avg new Product	Avg Medar	Avg new Product	Avg Medar
<i>DF2- Gulf of Lion</i>						
surface water (0-150db)	2.68±2.53(68)**	1.7±1.1	0.15±0.06(68)	0.13±0.04	2.91±1.33(68)	1.72±0.64
LIW core (S_{max} depth range: 300-500db)	8.49±0.18(17)	6.13±0.32	0.38±0.02(17)	0.34±0.01	8.67±0.69(17)	6.12±0.61
Deep water (>1500db)	8.03±0.43(33)	7.64±0.31	0.37±0.01(33)	0.37±0.015	8.7±0.67(33)	7.95±0.06
<i>DF3- Liguro-Provençal</i>						
surface water (0-150db)	2.31±2.4(205)	3.0±2.6	0.12±0.07(205)	0.19±0.05	2.45±1.05(205)	2.16±1.05
LIW core (S_{max} depth range: 300-500db)	8.05±0.18(76)	7.74±0.13	0.36±0.01(76)	0.35±0.01	7.49±0.55(76)	6.26±0.60
Deep water (>1500db)	8.18±0.25(142)	7.79±0.04	0.37±0.02(142)	1.03±1.29	8.98±0.39(142)	7.60±0.21
<i>DF4- Ligurian East</i>						
surface water (0-150db)	0.7±0.69(228)	0.61±1.03	0.05±0.02(228)	0.18±0.02	1.37±0.45(228)	1.27±1.86
LIW core (S_{max} depth range: 300-500db)	6.8±0.4(23)	5.54±0	0.3±0.02(21)	0.36±0.06	5.86±0.9(24)	4.86±0
Deep water (>1500db)	-	-	-	-	-	-
<i>DS2- Balearic Sea</i>						
surface water (0-150db)	1.32±1.46(196)	1.19±1.5	0.08±0.04(196)	0.11±0.04	1.61±0.64(196)	1.54±0.78
LIW core (S_{max} depth range: 300-500db)	8.32±0.32(58)	6.92±0.12	0.37±0.02(60)	0.39±0.003	7.31±0.9(60)	7.55±0.62
Deep water (>1500db)	8.2±0.35(88)	-	0.37±0.01(88)	-	8.71±0.51(88)	8.45±0.8
<i>DF1- Algero-Provençal</i>						
surface water (0-150db)	0.87±0.85(372)	1.08±1.7	0.05±0.02(372)	0.07±0.05	1.42±0.3(372)	1.28±0.73
LIW core (S_{max} depth range: 300-500db)	8.07±0.34(126)	7.51±0.18	0.36±0.02(126)	0.34±0.008	6.84±0.95(126)	5.96±0.77
Deep water (>1500db)	8.36±0.27(300)	7.87±0.13	0.38±0.02(300)	0.38±0.001	9.01±0.33(300)	8.18±0.10
<i>DS1- Alboran Sea</i>						
surface water (0-150db)	2.75±2.87(299)	2.51±2.23	0.17±0.11(299)	0.16±0.07	2.07±1.38(299)	2.31±1.14
LIW core (S_{max} depth range: 400-600db)	8.89±0.4(77)	8.14±0.11	0.42±0.02(77)	0.37±0.008	8.77±1.66(76)	7.95±0.34
Deep water (>1500db)	7.72±0.81(65)	-	0.36±0.04(65)	-	8.98±0.63(65)	8.16±0
<i>DS3- Algerian West</i>						
surface water (0-150db)	1.8±1.88(254)	1.82±2.01	0.11±0.05(354)	0.11±0.06	1.71±0.68(354)	2.10±0.91
LIW core (S_{max} depth range: 400-600db)	9.33±0.08(70)	8.28±0.15	0.41±0(73)	0.38±0.012	8.1±0.53(72)	6.68±0.80
Deep water (>1500db)	8.37±0.27(246)	8.047±0.013	0.37±0.02(246)	0.36±0.006	9.22±0.35(246)	8.87±0.23
<i>DS4- Algerian East</i>						
surface water (0-150db)	0.94±0.77(170)	0.75±1.26	0.07±0.02(170)	0.05±0.03	1.53±0.12(170)	1.35±0.52
LIW core (S_{max} depth range: 400-600db)	8.5±0.25(43)	8.60±0.06	0.38±0.03(43)	0.38±0.008	7.27±0.67(42)	7.092±0.55
Deep water (>1500db)	7.94±0.24(132)	8.06±0.06	0.36±0.02(132)	0.38±0.006	8.73±0.38(132)	9.04±0.24
<i>DT1- Tyrrhenian North</i>						
surface water (0-150db)	1.03±1.14(231)	0.88±1.2	0.06±0.02(231)	0.09±0.03	1.64±0.52(231)	2.19±0.59
LIW core (S_{max} depth range: 400-600db)	5.95±0.49(43)	5.86±0.36	0.27±0.03(44)	0.308±0.02	7.06±0.08(44)	6.76±0.59
Deep water (>1500db)	7.75±0.37(194)	7.12±0.47	0.36±0.03(194)	0.40±0.02	9.19±0.47(194)	7.51±0.49
<i>DT3- Tyrrhenian South</i>						
surface water (0-150db)	1.21±1.38(711)	1.23±1.80	0.06±0.03(711)	0.061±0.04	1.58±0.61(711)	1.55±1.05
LIW core (S_{max} depth range: 300-500db)	6.2±0.28(225)	6.42±0.01	0.26±0.02(225)	0.254±0.005	6.28±0.65(224)	6.68±0.44
Deep water (>1500db)	7.88±0.4(227)	7.12±0.26	0.37±0.02(227)	0.31±0.007	9.04±0.52(227)	8.02±0.07
<i>DII- Sardinia Channel</i>						
surface water (0-150db)	1.22±1.39(271)	1.42±1.95	0.07±0.03(271)	0.064±0.03	1.57±0.68(271)	1.39±1.01
LIW core (S_{max} depth range: 300-500db)	6.52±0.17(89)	6.45±0.22	0.27±0.02(89)	0.250±0.01	6.36±0.67(89)	6.27±0.70
Deep water (>1500db)	7.91±0.62(107)	-	0.37±0.03(107)	0.32±0	8.64±0.91(107)	-
<i>DI3- Sicily Strait</i>						
surface water (0-150db)	0.87±0.68(583)	0.77±0.81	0.06±0.02(583)	0.063±0.02	1.53±0.29(583)	1.44±0.58
LIW core (S_{max} depth range: 200-400db)	4.95±0.47(80)	5.14±0.14	0.21±0.02(78)	0.194±0.004	5.26±0.79(81)	6.744±0.41
Deep water (>1500db)	-	-	-	-	-	-

**Average (Avg) ± standard deviation of inorganic nutrient (the number observation within depth range) for three layers from the adjusted/new product and MEDATLAS vertical climatological profiles (called here Medar). Regions are defined according to Manca et al. (2004) (table 2S, Fig.2S)